Table 2.5.3.5. *Symmetries of hexagonal six-beam CBED patterns for diffraction groups*

		Projection diffraction group									
		31_R		$3m1_R$					61_R		
Diffraction group		3	31_R	$3m_R$		$3m$		$3m1_R$	6	6_R	61_R
Two-dimensional symmetry		3	3	3		$3m$		$3m$	6	3	6
Three-dimensional symmetry			m'	$2'$				m', $(2')$		i	m', (i)
Zone-axis pattern	Bright-field pattern	3	6	$3m$		$3m$		$6mm$	6	3	6
	Whole-field pattern	3	3	3		$3m$		$3m$	6	3	6
Hexagonal six-beam pattern	O	1	1	1	m_2	1	m_v	m_2	m_v	1	1	1
	G	1	1_R	m_2	1	1	m_v	1_R	$1_R m_v(m_2)$	1	1	1_R
	F	1	1	m_2	1	1	1	1	m_2	1	1	1
	S	1	1	1	m_2	1	1	m_2	1	1	1	1
	FF'	1	3_R	1	1	1	m_v	3_R	$3_R m_v$	1	1	3_R
	SS'	1	1	1	1	1	m_v	1	m_v	1	6_R	6_R
A pair of symmetrical six-beam patterns 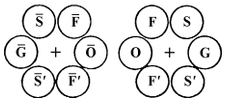	$\pm O$	1	1_R	m_2	1	m_v	1	$m_v 1_R$	$1_R m_2$	2	1	$2(1_R)$
	$\pm G$	1	1	1	m_R	m_v	1	$m_v m_R$	1	2	2_R	21_R
	$\pm F$	1	1	1	1	m_v	1	m_v	1	1	6_R	6_R
	$\pm S$	1	3_R	1	1	m_v	1	$3_R m_v$	3_R	1	1	3_R
	$F'\bar{F}$	1	1	1	m_R	1	1	m_R	1	2	1	2
	$S'\bar{S}$	1	1	m_R	1	1	1	1	m_R	2	1	2
Point group		23, 3	$\bar{6}$	432, 32		$\bar{4}3m$, $3m$		$\bar{6}m2$	6	$m3$, 3	$6/m$	

		Projection diffraction group				
		$6mm1_R$				
Diffraction group		$6m_R m_R$	$6mm$	$6_R mm_R$		$6mm1_R$
Two-dimensional symmetry		6	$6mm$	$3m$		$6mm$
Three-dimensional symmetry		$2'$		i, $(2')$		m', $(i, 2')$
Zone-axis pattern	Bright-field pattern	$6mm$	$6mm$	$3m$		$6mm$
	Whole-field pattern	6	$6mm$	$3m$		$6mm$
Hexagonal six-beam pattern	O	m_2	m_v	1	$m_v(m_2)$	$m_v(m_2)$
	G	m_2	m_v	m_2	m_v	$1_R m_v(m_2)$
	F	m_2	1	m_2	1	m_2
	S	m_2	1	1	m_2	m_2
	FF'	1	m_v	1	m_v	$3_R m_v$
	SS'	1	m_v	6_R	$6_R m_v$	$6_R m_v$
A pair of symmetrical six-beam patterns 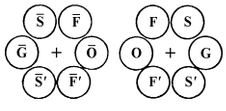	$\pm O$	$2m_2$	$2m_{v'}$	$m_v(m_2)$	1	$2(1_R)m_{v'}(m_2)$
	$\pm G$	$2m_R$	$2m_{v'}$	$2_R m_v$	$2_R m_R$	$21_R m_{v'}(m_R)$
	$\pm F$	1	$m_{v'}$	$6_R m_v$	6_R	$6_R m_{v'}$
	$\pm S$	1	$m_{v'}$	m_v	1	$3_R m_{v'}$
	$F'\bar{F}$	$2m_R$	2	1	m_R	$2m_R$
	$S'\bar{S}$	$2m_R$	2	m_R	1	$2m_R$
Point group		622	$6mm$	$m3m$, $\bar{3}m$		$6/mmm$

SMB pattern, and two-dimensional symmetry elements from a pair of SMB patterns, as shown in Tables 2.5.3.5, 2.5.3.6 and 2.5.3.7. Therefore, the use of a ZAP and SMB patterns is the most efficient way to find as many crystal symmetry elements in a specimen as possible.

2.5.3.3. Space-group determination

2.5.3.3.1. Lattice-type determination

When the point group of a specimen crystal is determined, the crystal axes may be found from a spot diffraction pattern recorded at a high-symmetry zone axis, using the orientations of the symmetry elements determined in the course of point-group determination. Integral-number indices are assigned to the spots of the diffraction patterns. The systematic absence of reflections indicates the lattice type of the crystal. It should be noted that reflections forbidden by the lattice type are always absent, even if dynamical diffraction takes place. (This is true for all sample thicknesses and accelerating voltages.) By comparing the experimentally obtained absences and the extinction rules known for the lattice types [P, C (A, B), I, F and R], a lattice type may be identified for the crystal concerned.

2.5.3.3.2. Identification of screw axes and glide planes

There are three space-group symmetry elements of diperiodic plane figures: (1) a horizontal screw axis $2'_1$, (2) a vertical glide plane g with a horizontal glide vector and (3) a horizontal glide plane g'. These are related to the point-group symmetry elements $2'$, m and m' of diperiodic plane figures, respectively. (It is noted that these symmetry elements and ten point-group symmetry elements form 80 space groups.)

Table 2.5.3.6. *Symmetries of square four-beam CBED patterns for diffraction groups*

			Projection diffraction group							
			41_R			$4mm1_R$				
Diffraction group			4	4_R	41_R	$4m_Rm_R$	$4mm$	4_Rmm_R		$4mm1_R$
Two-dimensional symmetry			4	(2)	4	4	$4mm$	($2mm$)		$4mm$
Three-dimensional symmetry				$\bar{4}$	m', (i, $\bar{4}$)	$2'$		$\bar{4}$, $2'$		m', (i, $2'$, $\bar{4}$)
Zone-axis pattern	Bright-field pattern		4	4	4	$4mm$	$4mm$	$4mm$		$4mm$
	Whole-field pattern		4	2	4	4	$4mm$	$2mm$		$4mm$
Square four-beam pattern		O	1	1	1	m_2	m_v	m_2	m_v	$m_v(m_2)$
		G	1	1	1_R	m_2	m_v	m_2	m_v	$1_Rm_v(m_2)$
		F	1	1	1	m_2	1	1	m_2	m_2
		FF'	1	4_R	4_R	1	m_v	4_R	4_Rm_v	4_Rm_v
Two pairs of square four-beam patterns 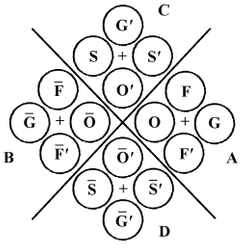	AB	$\pm O$	2	2	$2(1_R)$	$2m_2$	$2m_{v'}$	$2m_2$	$2m_{v'}$	$2(1_R)m_{v'}(m_2)$
		$\pm G$	2	2	21_R	$2m_R$	$2m_{v'}$	$2m_R$	$2m_{v'}$	$21_Rm_{v'}(m_R)$
		FF'	2	2	2	$2m_R$	2	2	$2m_R$	$2m_R$
		$\pm F$	1	4_R	4_R	1	$m_{v'}$	4_R	$4_Rm_{v'}$	$4_Rm_{v'}$
	AC	OO'	4	4	4	$4m_2$	$4m_{v''}$	$4m_v$	$4m_2$	$4m_{v''}(m_2)$
		GG'	4	4_R	41_R	$4m_R$	$4m_{v''}$	4_Rm_v	4_Rm_R	$41_Rm_{v''}(m_R)$
		FS	4	1	4	$4m_R$	4	m_R	1	$41_Rm_{v''}(m_R)$
		FS'	1	1	1_R	1	$m_{v''}$	m_v	1	$1_Rm_{v''}$
Point group			4	$\bar{4}$	$4/m$	432, 422	$4mm$	$\bar{4}3m$, $\bar{4}2m$		$m3m$, $4/mmm$

Table 2.5.3.7. *Symmetries of rectangular four-beam CBED patterns for diffraction groups*

			Projection diffraction group						
			$m1_R$			$2mm1_R$			
Diffraction group			m_R	m	$m1_R$	$2m_Rm_R$	$2mm$	2_Rmm_R	$2mm1_R$
Two-dimensional symmetry				m	m	2	$2mm$	m	$2mm$
Three-dimensional symmetry			$2'$		m', $2'$	$2'$		$2'$, i	m', $2'$, i
Zone-axis pattern	Bright-field pattern		m	m	$2mm$	$2mm$	$2mm$	m	$2mm$
	Whole-field pattern		1	m	m	2	$2mm$	m	$2mm$
Rectangular four-beam pattern		O	1	1	1	1	1	1	1
		G	1	1	1_R	1	1	1	1_R
		F	m_2	1	m_2	m_2	1	m_2	m_2
		S	1	1	1	m_2	1	1	m_2
Three pairs of rectangular four-beam patterns 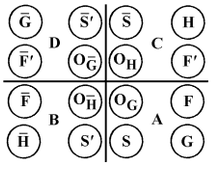	AB	$O_GO_{\bar{H}}$	m_2	1	m_2	m_2	m_v	$m_v(m_2)$	$m_v(m_2)$
		$G\bar{H}$	1	1	1	m_R	m_v	m_v	m_vm_R
		$F\bar{F}$	1	1	1	1	m_v	2_Rm_v	2_Rm_v
		SS'	1	1	1_R	1	m_v	m_v	m_v1_R
	AC	O_GO_H	1	m_v	m_v	m_2	$m_{v'}$	1	$m_{v'}(m_2)$
		GH	m_R	m_v	m_vm_R	m_R	$m_{v'}$	m_R	$m_{v'}m_R$
		FF'	1	m_v	m_v1_R	1	$m_{v'}$	1	$m_{v'}1_R$
		$S\bar{S}$	1	m_v	m_v	1	$m_{v'}$	2_R	$2_Rm_{v'}$
	AD	$O_GO_{\bar{G}}$	1	1	1_R	2	2	1	$2(1_R)$
		GG	1	1	1	2	2	2_R	21_R
		$F\bar{F}'$	1	1	1	$2m_R$	2	1	$2m_R$
		$S\bar{S}'$	m_R	1	m_R	$2m_R$	2	m_R	$2m_R$
Point group			2, 222, $mm2$, 4, $\bar{4}$, 422, $4mm$, $\bar{4}2m$, 32, $\bar{6}$, 622, $6mm$, $\bar{6}m2$, 23, 432, $\bar{4}3m$	m, $mm2$, $4mm$, $\bar{4}2m$, $3m$, $\bar{6}$, $6mm$, $\bar{6}m2$, $\bar{4}3m$	$mm2$, $4mm$, $42m$, $6mm$, $\bar{6}m2$, $\bar{4}3m$	222, 422, $\bar{4}2m$, 622, 23, 432	$mm2$, $\bar{6}m2$	$2/m$, mmm, $4/m$, $4/mmm$, $\bar{3}m$, $\bar{6}/m$, $6/mmm$, $m3$, $m3m$	mmm, $4/mmm$, $m3$, $m3m$, $6/mmm$

The ordinary extinction rules for screw axes and glide planes hold only in the approximation of kinematical diffraction. The kinematically forbidden reflections caused by these symmetry elements appear owing to *Umweganregung* of dynamical diffraction. Extinction of intensity, however, does take place in these reflections at certain crystal orientations with respect to the incident beam (*i.e.* in certain regions within a CBED disc). This dynamical extinction was first predicted by Cowley & Moodie (1959) and was discussed by Miyake *et al.* (1960) and Cowley *et al.* (1961). Goodman & Lehmpfuhl (1964) first observed the dynamical extinction as dark cross lines in kinematically forbidden reflection discs of CBED patterns of CdS. Gjønnes & Moodie

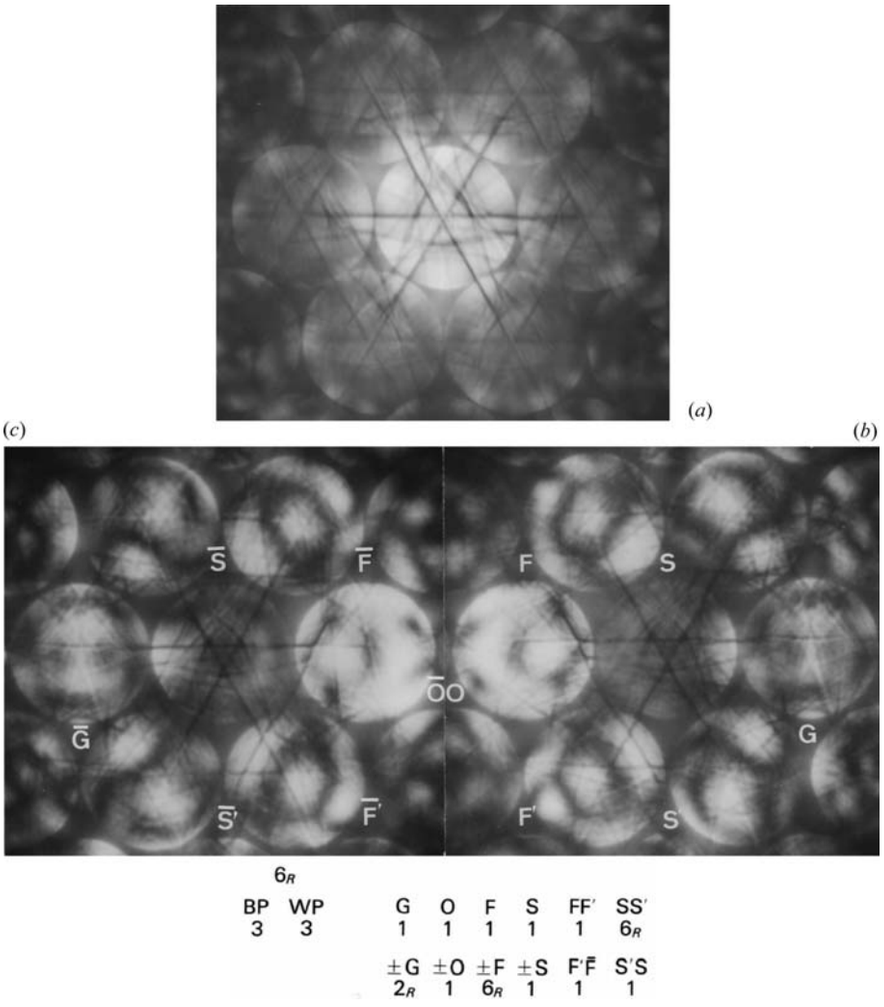

Fig. 2.5.3.8. CBED patterns of FeS_2 taken with the [111] incidence. (*a*) Zone-axis pattern, (*b*) hexagonal six-beam pattern with excitation of reflection $+G$, (*c*) hexagonal six-beam pattern with excitation of reflection $-G$. Symmetry 6_R is noted between discs S and S' and discs $\bar{F}$ and $\bar{F}'$.

(1965) discussed the dynamical extinction in a more general way considering not only ZOLZ reflections but also HOLZ reflections. They completely clarified the dynamical extinction rules by considering the exact cancellation which may occur along certain symmetry-related multiple-scattering paths. Based on the results of Gjønnes & Moodie (1965), Tanaka, Sekii & Nagasawa (1983) tabulated the dynamical extinctions expected at all the possible crystal orientations for all the space groups. These were later tabulated in a better form on pages 162 to 172 of the book by Tanaka & Terauchi (1985).

Fig. 2.5.3.10(*a*) illustrates *Umweganregung* paths to a kinematically forbidden reflection. The $0k0$ (k = odd) reflections are kinematically forbidden because a b-glide plane exists perpendicular to the a axis and/or a 2_1 screw axis exists in the b direction. Let us consider an *Umweganregung* path a in the zeroth-order Laue zone to the 010 forbidden reflection and path b which is symmetric to path a with respect to axis k. Owing to the translation of one half of the lattice parameter b caused by the glide plane and/or the 2_1 screw axis, the following relations hold between the crystal structure factors:

$$F(h,k) = F(\bar{h},k) \quad \text{for } k = 2n,$$
$$F(h,k) = -F(\bar{h},k) \quad \text{for } k = 2n+1. \qquad (2.5.3.1)$$

That is, the structure factors of reflections $hk0$ and $\bar{h}k0$ have the same phase for even k but have opposite phases for odd k.

Since an *Umweganregung* path to the kinematically forbidden reflection $0k0$ contains an odd number of reflections with odd k, the following relations hold:

$$F(h_1,k_1)F(h_2,k_2)\ldots F(h_n,k_n) \quad \text{for path } a$$
$$= -F(\bar{h}_1,k_1)F(\bar{h}_2,k_2)\ldots F(\bar{h}_n,k_n) \quad \text{for path } b, \qquad (2.5.3.2)$$

where

$$\sum_{i=1}^{n} h_i = 0, \quad \sum_{i=1}^{n} k_i = k \ (k = \text{odd})$$

and the functions including the excitation errors are omitted because only the cases in which the functions are the same for all the paths are considered. The excitation errors for paths a and b become the same when the projection of the Laue point along the zone axis concerned, L, lies on axis k. Since the two waves passing through paths a and b have the same amplitude but opposite signs, these waves are superposed on the $0k0$ discs (k = odd) and cancel out, resulting in dark lines A in the forbidden discs, as shown in Fig. 2.5.3.10(*b*). The line A runs parallel to axis k passing through the projection point of the zone axis.

In path c, the reflections are arranged in the reverse order to those in path b. When the 010 reflection is exactly excited, two paths a and c are symmetric with respect to the bisector m'–m' of

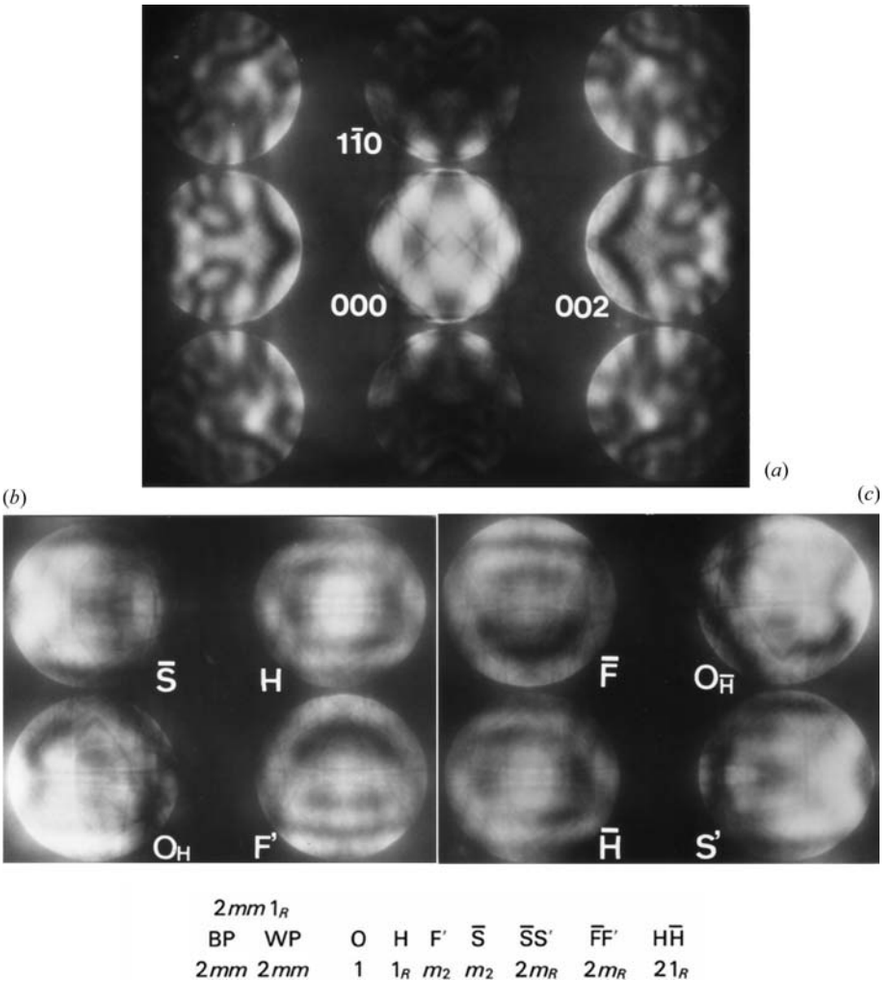

Fig. 2.5.3.9. CBED patterns of V_3Si taken with the [110] incidence. (*a*) Zone-axis pattern, (*b*) rectangular four-beam pattern with excitation of reflections H, $\bar{S}$ and F, (*c*) rectangular four-beam pattern with excitation of reflections $\bar{H}$, S and $\bar{F}$.

the 010 vector having the same excitation errors. The following equation holds:

$$F(h_1, k_1)F(h_2, k_2)\ldots F(h_n, k_n) \quad \text{for path } a$$
$$= -F(\bar{h}_n, k_n)F(\bar{h}_{n-1}, k_{n-1})\ldots F(\bar{h}_1, k_1) \quad \text{for path } c. \tag{2.5.3.3}$$

Since the waves passing through these paths have the same amplitude but opposite signs, these waves are superposed on the 010 discs and cancel out, resulting in dark line B in this disc, as shown in Fig. 2.5.3.10(*b*). Line B appears perpendicular to line A at the exact Bragg positions. When *Umweganregung* paths are present only in the zeroth-order Laue zone, the glide plane and screw axis produce the same dynamical extinction lines A and B. We call these lines A_2 and B_2 lines, subscript 2 indicating that the *Umweganregung* paths lie in the zeroth-order Laue zone.

The dynamical extinction effect is analogous to interference phenomena in the Michelson interferometer. That is, the incident beam is split into two beams by Bragg reflections in a crystal. These beams take different paths, in which they suffer a relative phase shift of π and are finally superposed on a kinematically forbidden reflection to cancel out.

When the paths include higher-order Laue zones, the glide plane produces only extinction lines A but the screw axis causes only extinction lines B. These facts are attributed to the different relations between structure factors for a 2_1 screw axis and a glide plane,

$$F(hkl) = (-1)^k F(\bar{h}k\bar{l}) \quad \text{for a } 2_1 \text{ screw axis in the [010] direction,} \tag{2.5.3.4}$$

$$F(hkl) = (-1)^k F(\bar{h}kl) \quad \text{for a } b \text{ glide in the (100) plane.} \tag{2.5.3.5}$$

In the case of the glide plane, extinction lines A are still formed because two waves passing through paths a and b have opposite signs to each other according to equation (2.5.3.5), but extinction lines B are not produced because equation (2.5.3.4) holds only for the 2_1 screw axis. In the case of the 2_1 screw axis, only the waves passing through paths a and c have opposite signs according to equation (2.5.3.4), forming extinction lines B only. We call these lines A_3 and B_3 dynamical extinction lines, suffix 3 indicating the *Umweganregung* paths being *via* higher-order Laue zones.

It was predicted by Gjønnes & Moodie (1965) that a horizontal glide plane g' gives a dark spot at the crossing point between extinction lines A and B (Fig. 2.5.3.10*b*) due to the cancellation between the waves passing through paths b and c. Tanaka, Terauchi & Sekii (1987) observed this dynamical extinction, though it appeared in a slightly different manner to that predicted by Gjønnes & Moodie (1965). Table 2.5.3.8 summarizes the appearance of the dynamical extinction lines for the glide planes g and g' and the 2_1 screw axis. The three space-group symmetry elements can be identified from the observed extinctions because these three symmetry elements produce different kinds of dynamical extinctions.

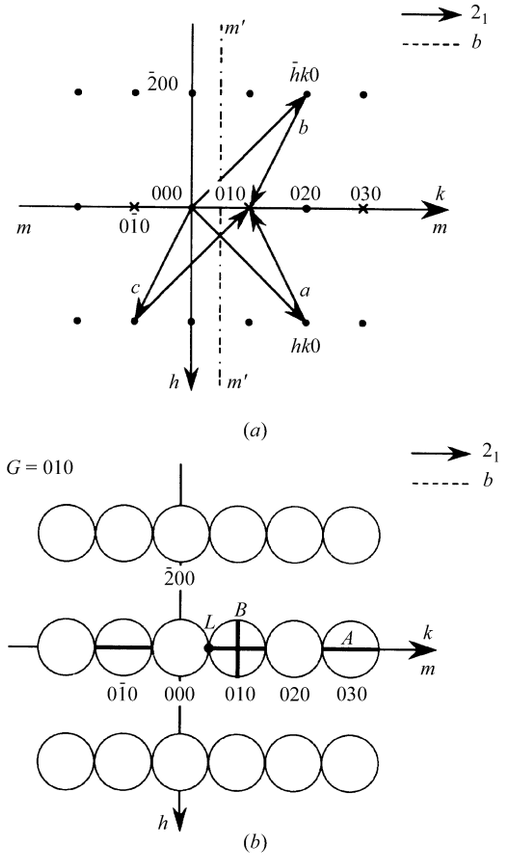

Fig. 2.5.3.10. Illustration of the production of dynamical extinction lines in kinematically forbidden reflections due to a b-glide plane and a 2_1 screw axis. (a) *Umweganregung* paths a, b and c. (b) Dynamical extinction lines A are formed in forbidden reflections $0k0$ (k = odd). Extinction line B perpendicular to the lines A is formed in the exactly excited 010 reflection.

In principle, a horizontal screw axis and a vertical glide plane can be distinguished by observations of the extinction lines A_3 and B_3. It is, however, not easy to observe the extinction lines A_3 and B_3 because broad extinction lines A_2 and B_2 appear at the same time. The presence of the extinction lines A_3 and B_3 can be revealed by inspecting the symmetries of fine defect HOLZ lines appearing in the forbidden reflections instead of by direct observation of the lines A_3 and B_3 (Tanaka, Sekii & Nagasawa, 1983). That is, if HOLZ lines form lines A_3 and B_3, HOLZ lines are symmetric with respect to the extinction lines A_2 and B_2. If HOLZ lines do not form lines A_3 and B_3, HOLZ lines are asymmetric with respect to the extinction lines A_2 and B_2. When the HOLZ lines are symmetric about the extinction lines A_2, the specimen crystal has a glide plane. When the HOLZ lines are symmetric with respect to lines B_2, a 2_1 screw axis exists. It should

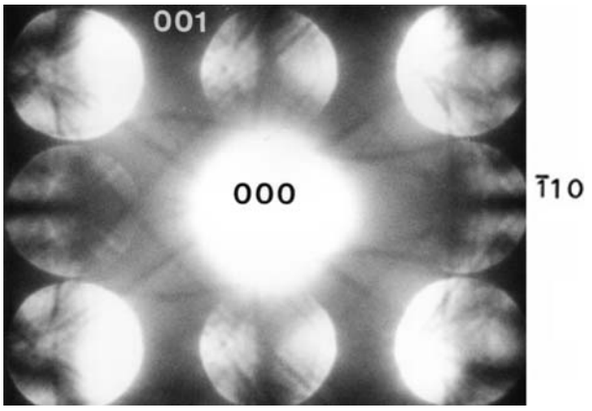

Fig. 2.5.3.12. CBED pattern of FeS_2 taken with the [110] electron-beam incidence. In the 001 and $00\bar{1}$ discs, HOLZ lines are asymmetric with respect to extinction lines A_2, indicating the existence of a 2_1 screw axis parallel to the c axis. In the $\bar{1}10$ and $1\bar{1}0$ discs, HOLZ lines are symmetric with respect to extinction lines A_2, indicating existence of a glide plane perpendicular to the c axis.

be noted that a relatively thick specimen area has to be selected to observe HOLZ lines in ZOLZ reflection discs.

Fig. 2.5.3.11 shows CBED patterns taken from (a) thin and (b) thick areas of FeS_2, whose space group is $P2_1/a\bar{3}$, at the 001 Bragg setting with the [100] electron-beam incidence. In the case of the thin specimen (Fig. 2.5.3.11a), only the broad dynamical extinction lines formed by the interaction of ZOLZ reflections are seen in the odd-order discs. On the other hand, fine HOLZ lines are clearly seen in the thick specimen (Fig. 2.5.3.11b). The HOLZ lines are symmetric with respect to both A_2 and B_2 extinction lines. This fact proves the presence of the extinction lines A_3 and B_3, or both the c glide in the (010) plane and the 2_1 screw axis in the c direction, this fact being confirmed by consulting Table 2.5.3.9. Fig. 2.5.3.12 shows a [110] zone-axis CBED pattern of FeS_2. A_2 extinction lines are seen in both the 001 and $\bar{1}10$ discs. Fine HOLZ lines are symmetric with respect to the A_2 extinction lines in the $\bar{1}10$ disc but asymmetric about the A_2 extinction line in the 001 disc, indicating formation of the A_3 extinction line only in the $\bar{1}10$ disc. This proves the existence of a 2_1 screw axis in the [001] direction and an a glide in the (001) plane. The appearance of HOLZ lines is easily changed by a change of a few hundred volts in the accelerating voltage. Steeds & Evans (1980) demonstrated for spinel changes in the appearance of HOLZ lines in the ZOLZ discs at accelerating voltages around 100 kV.

Another practical method for distinguishing between glide planes and 2_1 screw axes is that reported by Steeds *et al.* (1978). The method is based on the fact that the extinction lines are observable even when a crystal is rotated with a glide plane kept parallel and with a 2_1 screw axis perpendicular to the incident

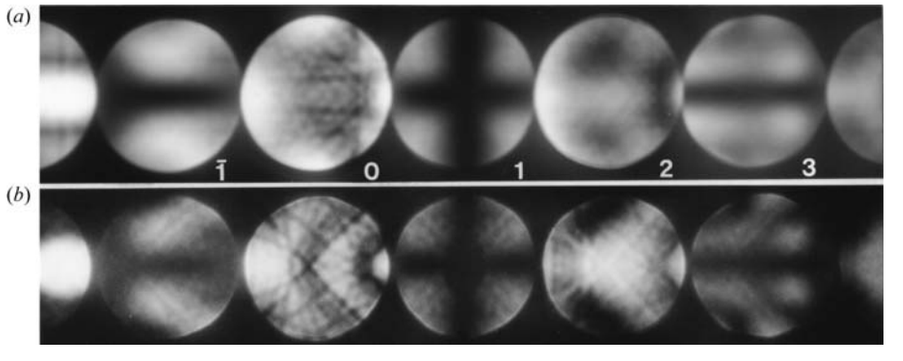

Fig. 2.5.3.11. CBED patterns obtained from (a) thin and (b) thick areas of (001) FeS_2. (a) Dynamical extinction lines A_2 and B_2 are seen. (b) Extinction lines A_3 and B_3 as well as A_2 and B_2 are formed because HOLZ lines are symmetric about lines A_2 and B_2.

Table 2.5.3.8. *Dynamical extinction rules for an infinitely extended parallel-sided specimen*

Symmetry elements of plane-parallel specimen	Orientation to specimen surface	Dynamical extinction lines	
		Two-dimensional (zeroth Laue zone) interaction	Three-dimensional (HOLZ) interaction
Glide planes	perpendicular: g	A_2 and B_2	A_3
	parallel: g'	—	intersection of A_3 and B_3
Twofold screw axis	perpendicular: 2_1	—	—
	parallel: $2_1'$	A_2 and B_2	B_3

beam. With reference to Fig. 2.5.3.10(*a*), extinction lines A_3 produced by a glide plane remain even when the crystal is rotated with respect to axis h but the lines are destroyed by a rotation of the crystal about axis k. Extinction lines B_3 originating from a 2_1 screw axis are not destroyed by a crystal rotation about axis k but the lines are destroyed by a rotation with respect to axis h.

2.5.3.3.3. Space-group determination

We now describe a space-group determination method which uses the dynamical extinction lines caused by the horizontal screw axis $2_1'$ and the vertical glide plane g of an infinitely extended parallel-sided specimen. We do not use the extinction due to the glide plane g' because observation of the extinction requires a laborious experiment. It should be noted that a vertical glide plane with a glide vector not parallel to the specimen surface cannot be a symmetry element of a specimen of finite thickness; however, the component of the glide vector perpendicular to the incident beam acts as a symmetry element g. (Which symmetry elements are observed by CBED is discussed in Section 2.5.3.3.5.) The 2_1, 4_1, 4_3, 6_1, 6_3 and 6_5 screw axes of crystal space groups that are set perpendicular to the incident beam act as a symmetry element $2_1'$ because two or three successive operations of 4_1, 4_3, 6_1, 6_3 and 6_5 screw axes make them equivalent to a 2_1 screw axis: $(4_1)^2 = (4_3)^2 = (6_1)^3 = (6_3)^3 = (6_5)^3 = 2_1$. The 4_2, 3_1, 3_2, 6_2 and 6_4 screw axes that are set perpendicular to the incident beam do not produce dynamical extinction lines because the 4_2 screw axis acts as a twofold rotation axis due to the relation $(4_2)^2 = 2$, the 3_1 and 3_2 screw axes give no specific symmetry in CBED patterns, and the 6_2 and 6_4 screw axes are equivalent to 3_1 and 3_2 screw axes due to the relations $(6_2)^2 = 3_2$ and $(6_4)^2 = 3_1$. Modifications of the dynamical extinction rules were investigated by Tanaka, Sekii & Nagasawa (1983) when more than one crystal symmetry element (that gives rise to dynamical extinction lines) coexists and when the symmetry elements are combined with various lattice types. Using these results, dynamical extinction lines A_2, A_3, B_2 and B_3 expected from all the possible crystal settings for all the space groups were tabulated.

Table 2.5.3.9 shows all the dynamical extinction lines appearing in the kinematically forbidden reflections for all the possible crystal settings of all the space groups. The first column gives space groups. In each of the following pairs of columns, the left-hand column of the pair gives the reflection indices and the symmetry elements causing the extinction lines and the right-hand column gives the types of the extinction lines. The (second) suffixes 1, 2 and 3 of a 2_1 screw axis in each column distinguish the first, the second and the third screw axis of the space group (as in the symbols 2_{11} and 2_{12} of space group $P2_12_12$). The glide symbols in the [001] column for space group $P4/nnc$ have two suffixes (n_{21} and n_{22}). The first suffix 2 denotes the second glide plane of the space group. The second suffixes 1 and 2, which appear in the tetragonal and cubic systems, distinguish two equivalent glide planes which lie in the x and y planes. The equivalent planes are distinguished only for the cases of [100], [010] and [001] electron-beam incidences, for convenience. The c-glide planes of space group $Pcc2$ are distinguished with symbols c_1 and c_2 (the first suffix only), because the equivalent planes do not exist. The glide symbol in the [001] column for space group $P4/mbm$ has only one suffix 1 or 2. The suffix distinguishes the equivalent glide planes lying in the x and y planes. The first suffix to distinguish the first and the second glide planes is not necessary because the space group has only one glide symbol b. When the index of the incident-beam direction is expressed with a symbol like $[h0l]$ for point groups 2, m and $2/m$, the index h or l can take a value of zero. That is, the extinction rules are applicable to the [100] and [001] electron-beam incidences. However, if columns for [100], [010] and [001] incidences are present, as in the case of point group $mm2$, $[hk0]$, $[0kl]$ and $[h0l]$ incidences are only for nonzero h, k and l. The reflections in which the extinction lines appear are always perpendicular to the corresponding incident-beam directions ($0k'l' \perp [0kl]$, $h'k'0 \perp [hk0]$, ...). The indices of the reflections in which extinction lines appear are odd if no remark is given. For c-glide planes of space groups $R3c$ and $R\bar{3}c$ and for d-glide planes, the reflections in which extinction lines appear are specified as $6n + 3$ and $4n + 2$ orders, respectively.

The number of indistinguishable space groups was first counted by Tanaka, Sekii & Nagasawa (1983) but later corrections were made by Eades & Spence (1987). It was found that 177 space groups out of 230 can be identified using the extinction lines (Tanaka *et al.*, 2002). Another reference for space-group determination is due to Eades (1988). The indistinguishable space-group sets using the extinction lines are listed in Table 2.5.3.10. Most of the sets are caused by the fact that CBED cannot identify 4_2, 3_1 (3_2) and 6_2 (6_4) screw axes. However, these sets can be rather easily distinguished in the ordinary way, that is, by observing how the intensities of the reflections which may be kinematically forbidden change when the crystal orientation is varied. If the axis concerned is a screw axis, kinematically forbidden reflections show a sudden decrease in intensity when an orientation change causes the loss of *Umweganregung* paths. If the axis is a rotation axis, the intensities of the reflections do not change conspicuously for such an orientation change. Using this test, each space group in the 23 sets can be identified except the pairs in parentheses and pairs (16) and (17) in Table 2.5.3.10 (see Eades, 1988).

Tsuda *et al.* (2000) showed theoretically that the coherent CBED method can distinguish between space groups ($I23$ and $I2_13$) and between ($I222$ and $I2_12_12_1$), which are indistinguishable pairs (16) and (17), respectively, in Table 2.5.3.10. The coherent CBED pattern is obtained in such a way that the convergence angle of the incident beam is set to a larger value than usual to make adjacent CBED discs overlap (Dowell & Goodman, 1973). When the focus point is displaced from the specimen, or a certain area is illuminated, sinusoidal interference fringes of the lattice spacing corresponding to the adjacent discs are formed in the overlapping regions if the probe size of the incident beam is smaller than the lattice spacing. (If the focus point of the incident beam is on the specimen, each overlapping region of the CBED discs shows uniform intensity.) Formation of the interference fringes was explained in detail first by Spence & Cowley (1978). Vine *et al.* (1992) showed distortion-free interference fringes from 6*H*-SiC and succeeded in observing the fringes with a shift of half a period due to a glide plane. Tsuda *et al.*'s method

Table 2.5.3.9. *Dynamical extinction lines appearing in ZOLZ reflections for all crystal space groups except Nos. 1 and 2*

Point groups 2, *m*, 2/*m* (second setting, unique axis *b*)

Space group		Incident-beam direction [*h*0*l*]
3	*P*2	
4	*P*2$_1$	0*k*0 A_2 B_2 2$_1$ B_3
5	*C*2	
6	*Pm*	
7	*Pc*	*h*0*l*$_o$ A_2 B_2 *c* A_3
8	*Cm*	
9	*Cc*	*h*$_e$0*l*$_o$ A_2 B_2 *c* A_3
10	*P*2/*m*	
11	*P*2$_1$/*m*	0*k*0 A_2 B_2 2$_1$ B_3
12	*C*2/*m*	
13	*P*2/*c*	*h*0*l*$_o$ A_2 B_2 *c* A_3
14	*P*2$_1$/*c*	0*k*0 A_2 B_2 2$_1$ B_3
		*h*0*l*$_o$ A_2 B_2 *c* A_3
15	*C*2/*c*	*h*$_e$0*l*$_o$ A_2 B_2 *c* A_3

Point group 222

Space group		Incident-beam direction [100]	[010]	[001]	[*hk*0]	[0*kl*]	[*h*0*l*]
16	*P*222						
17	*P*222$_1$	00*l* A_2 B_2 2$_1$ B_3	00*l* A_2 B_2 2$_1$ B_3		00*l* A_2 B_2 2$_1$ B_3		
18	*P*2$_1$2$_1$2	0*k*0 A_2 B_2 2$_{12}$ B_3	*h*00 A_2 B_2 2$_{11}$ B_3	*h*00 A_2 B_2 2$_{11}$ B_3 0*k*0 2$_{12}$		*h*00 A_2 B_2 2$_{11}$ B_3	0*k*0 A_2 B_2 2$_{12}$ B_3
19	*P*2$_1$2$_1$2$_1$	0*k*0 A_2 B_2 2$_{12}$ B_3 00*l* 2$_{13}$	*h*00 A_2 B_2 2$_{11}$ B_3 00*l* 2$_{13}$	*h*00 A_2 B_2 2$_{11}$ B_3 0*k*0 2$_{12}$	00*l* A_2 B_2 2$_{13}$ B_3	*h*00 A_2 B_2 2$_{11}$ B_3	0*k*0 A_2 B_2 2$_{12}$ B_3
20	*C*222$_1$	00*l* A_2 B_2 2$_1$ B_3	00*l* A_2 B_2 2$_1$ B_3		00*l* A_2 B_2 2$_1$ B_3		
21	*C*222						
22	*F*222						
23	*I*222						
24	*I*2$_1$2$_1$2$_1$						

Point group *mm*2

Space group		Incident-beam direction [100]	[010]	[001]	[*hk*0]	[0*kl*]	[*h*0*l*]
25	*Pmm*2						
26	*Pmc*2$_1$	00*l* A_2 B_2 *c*, 2$_1$ A_3 B_3	00*l* 2$_1$ B_3		00*l* A_2 B_2 2$_1$ B_3		*h*0*l*$_o$ A_2 B_2 *c* A_3
27	*Pcc*2	00*l* *c*$_2$ A_3	00*l* *c*$_1$ A_3			0*kl*$_o$ A_2 B_2 *c*$_1$ A_3	*h*0*l*$_o$ A_2 B_2 *c*$_2$ A_3
28	*Pma*2			*h*00 A_2 B_2 *a* A_3			*h*$_o$0*l* A_2 B_2 *a* A_3
29	*Pca*2$_1$	00*l* 2$_1$ B_3	00*l* A_2 B_2 *c*, 2$_1$ A_3 B_3	*h*00 A_2 B_2 *a* A_3	00*l* A_2 B_2 2$_1$ B_3	0*kl*$_o$ A_2 B_2 *c* A_3	*h*$_o$0*l* A_2 B_2 *a* A_3

Table 2.5.3.9 (*cont.*)

Space group	Incident-beam direction					
	[100]	[010]	[001]	[*hk*0]	[0*kl*]	[*h*0*l*]
30 *Pnc*2	00*l* *c* A_3	00*l* *n* A_3	0*k*0 A_2 B_2 *n* A_3		0*kl*: A_2 B_2 $k + l =$ A_3 $2n + 1$ *n*	$h0l_o$ A_2 B_2 *c* A_3
31 *Pmn*2_1	00*l* A_2 B_2 *n*, 2_1 A_3 B_3	00*l* 2_1 B_3	*h*00 A_2 B_2 *n* A_3	00*l* A_2 B_2 2_1 B_3		*h*0*l*: A_2 B_2 $h + l =$ A_3 $2n + 1$ *n*
32 *Pba*2			*h*00 A_2 B_2 *a* A_3 0*k*0 *b*		$0k_ol$ A_2 B_2 *b* A_3	h_o0l A_2 B_2 *a* A_3
33 *Pna*2_1	00*l* 2_1 B_3	00*l* A_2 B_2 *n*, 2_1 A_3 B_3	*h*00 A_2 B_2 *a* A_3 0*k*0 *n*	00*l* A_2 B_2 2_1 B_3	0*kl*: A_2 B_2 $k + l =$ A_3 $2n + 1$ *n*	h_o0l A_2 B_2 *a* A_3
34 *Pnn*2	00*l* n_2 A_3	00*l* n_1 A_3	*h*00 A_2 B_2 n_2 A_3 0*k*0 n_1		0*kl*: A_2 B_2 $k + l =$ A_3 $2n + 1$ n_1	*h*0*l*: A_2 B_2 $h + l =$ A_3 $2n + 1$ n_2
35 *Cmm*2 *ba*2						
36 *Cmc*2_1 *bn*2_1	00*l* A_2 B_2 *c*, 2_1 A_3 B_3	00*l* 2_1 B_3		00*l* A_2 B_2 2_1 B_3		h_e0l_o A_2 B_2 *c* A_3
37 *Ccc*2 *nn*2	00*l* c_2 A_3	00*l* c_1 A_3			$0k_el_o$ A_2 B_2 c_1 A_3	h_e0l_o A_2 B_2 c_2 A_3
38 *Amm*2 *nc*2_1						
39 *Abm*2 *cc*2_1					$0k_ol_o$ A_2 B_2 *b* A_3	
40 *Ama*2 *nn*2_1			*h*00 A_2 B_2 *a* A_3			h_o0l_e A_2 B_2 *a* A_3
41 *Aba*2 *cn*2_1			*h*00 A_2 B_2 *a* A_3		$0k_ol_o$ A_2 B_2 *b* A_3	h_o0l_e A_2 B_2 *a* A_3
42 *Fmm*2						
43 *Fdd*2 *dd*2_1	00*l*: $l = 4n + 2$ A_3 d_2	00*l*: $l = 4n + 2$ A_3 d_1	*h*00: A_2 B_2 $h = 4n + 2$ A_3 d_2 0*k*0: $k = 4n + 2$ d_1		$0k_el_e$: A_2 B_2 $k_e + l_e =$ A_3 $4n + 2$ d_1	h_e0l_e: A_2 B_2 $h_e + l_e =$ A_3 $4n + 2$ d_2
44 *Imm*2 *nn*2_1						
45 *Iba*2 *cc*2_1					$0k_ol_o$ A_2 B_2 *b* A_3	h_o0l_o A_2 B_2 *a* A_3
46 *Ima*2 *nc*2_1						h_o0l_o A_2 B_2 *a* A_3

Point group *mmm*

Space group	Incident-beam direction					
	[100]	[010]	[001]	[*hk*0]	[0*kl*]	[*h*0*l*]
47 *P*2/*m*2/*m*2/*m*						
48 *P*2/*n*2/*n*2/*n*	00*l* n_2 A_3 0*k*0 n_3	00*l* n_1 A_3 *h*00 n_3	0*k*0 n_1 A_3 *h*00 n_2	*hk*0: A_2 B_2 $h + k =$ A_3 $2n + 1$ n_3	0*kl*: A_2 B_2 $k + l =$ A_3 $2n + 1$ n_1	*h*0*l*: A_2 B_2 $h + l =$ A_3 $2n + 1$ n_2
49 *P*2/*c*2/*c*2/*m*	00*l* c_2 A_3	00*l* c_1 A_3			$0kl_o$ A_2 B_2 c_1 A_3	$h0l_o$ A_2 B_2 c_2 A_3
50 *P*2/*b*2/*a*2/*n*	0*k*0 *n* A_3	*h*00 *n* A_3	0*k*0 *b* A_3 *h*00 *a*	*hk*0: A_2 B_2 $h + k =$ A_3 $2n + 1$ *n*	$0k_ol$ A_2 B_2 *b* A_3	h_o0l A_2 B_2 *a* A_3
51 $P2_1$/*m*2/*m*2/*a*		*h*00 A_2 B_2 2_1, *a* A_3 B_3	*h*00 2_1 B_3	h_ok0 A_2 B_2 *a* A_3	*h*00 A_2 B_2 2_1 B_3	

Table 2.5.3.9 (*cont.*)

Space group	Incident-beam direction					
	[100]	[010]	[001]	[*hk*0]	[0*kl*]	[*h*0*l*]
52 *P*2/*n*2$_1$/*n*2/*a*	00*l* n_2 A_3	00*l* n_1 A_3 *h*00 *a*	0*k*0 n_1, 2$_1$ A_2 A_3 B_2 B_3	$h_o k0$ *a* A_2 A_3 B_2	0*kl*: $k + l =$ $2n + 1$ n_1 A_2 A_3 B_2	*h*0*l*: $h + l =$ $2n + 1$ n_2 A_2 A_3 B_2
	0*k*0 2$_1$ B_3		*h*00 n_2 A_3			0*k*0 2$_1$ A_2 B_2 B_3
53 *P*2/*m*2/*n*2$_1$/*a*	00*l* n, 2$_1$ A_2 A_3 B_2 B_3	*h*00 *a* A_3	*h*00 *n* A_3	$h_o k0$ *a* A_2 A_3 B_2		*h*0*l*: $h + l =$ $2n + 1$ n A_2 A_3 B_2
		00*l* 2$_1$ B_3		00*l* 2$_1$ A_2 B_2 B_3		
54 *P*2$_1$/*c*2/*c*2/*a*	00*l* c_2 A_3	00*l* c_1 A_3	*h*00 2$_1$ B_3	$h_o k0$ *a* A_2 A_3 B_2	0*kl*$_o$ c_1 A_2 A_3 B_2	*h*0*l*$_o$ c_2 A_2 A_3 B_2
		*h*00 *a*, 2$_1$ A_2 A_3 B_2 B_3			*h*00 2$_1$ A_2 B_2 B_3	
55 *P*2$_1$/*b*2$_1$/*a*2/*m*	0*k*0 2$_{12}$ B_3	*h*00 2$_{11}$ B_3	0*k*0 *b*, 2$_{12}$ A_2 A_3 B_2 B_3		0*k*$_o$*l* *b* A_2 A_3 B_2	*h*$_o$0*l* *a* A_2 A_3 B_2
			*h*00 *a*, 2$_{11}$		*h*00 2$_{11}$ A_2 B_2 B_3	0*k*0 2$_{12}$ A_2 B_2 B_3
56 *P*2$_1$/*c*2$_1$/*c*2/*n*	00*l* c_2 A_3	00*l* c_1 A_3	0*k*0 2$_{12}$ B_3 *h*00 2$_{11}$	*hk*0: $h + k =$ $2n + 1$ n A_2 A_3 B_2	0*kl*$_o$ c_1 A_2 A_3 B_2	*h*0*l*$_o$ c_2 A_2 A_3 B_2
	0*k*0 2$_{12}$, n A_2 A_3 B_2 B_3	*h*00 2$_{11}$, n A_2 A_3 B_2 B_3			*h*00 2$_{11}$ A_2 B_2 B_3	0*k*0 2$_{12}$ A_2 B_2 B_3
57 *P*2/*b*2$_1$/*c*2$_1$/*m*	00*l* c, 2$_{12}$ A_2 A_3 B_2 B_3	00*l* 2$_{12}$ B_3	0*k*0 *b*, 2$_{11}$ A_2 A_3 B_2 B_3	00*l* 2$_{12}$ A_2 B_2 B_3	0*k*$_o$*l* *b* A_2 A_3 B_2	*h*0*l*$_o$ c A_2 A_3 B_2
	0*k*0 2$_{11}$ B_3					0*k*0 2$_{11}$ A_2 B_2 B_3
58 *P*2$_1$/*n*2$_1$/*n*2/*m*	00*l* n_2 A_3	00*l* n_1 A_3	0*k*0 n_1, 2$_{12}$ A_2 A_3 B_2 B_3 *h*00 n_2, 2$_{11}$		0*kl*: $k + l =$ $2n + 1$ n_1 A_2 A_3 B_2	*h*0*l*: $h + l =$ $2n + 1$ n_2 A_2 A_3 B_2
	0*k*0 2$_{12}$ B_3	*h*00 2$_{11}$ B_3			*h*00 2$_{11}$ A_2 B_2 B_3	0*k*0 2$_{12}$ A_2 B_2 B_3
59 *P*2$_1$/*m*2$_1$/*m*2/*n*	0*k*0 n, 2$_{12}$ A_2 A_3 B_2 B_3	*h*00 n, 2$_{11}$ A_2 A_3 B_2 B_3	0*k*0 2$_{12}$ B_3 *h*00 2$_{11}$	*hk*0: $h + k =$ $2n + 1$ n A_2 A_3 B_2	*h*00 2$_{11}$ A_2 B_2 B_3	0*k*0 2$_{12}$ A_2 B_2 A_3
60 *P*2$_1$/*b*2/*c*2$_1$/*n*	00*l* c, 2$_{12}$ A_2 A_3 B_2 B_3	*h*00 n, 2$_{11}$ A_2 A_3 B_2 B_3	0*k*0 *b* A_3	*hk*0: $h + k =$ $2n + 1$ n A_2 A_3 B_2	0*k*$_o$*l* *b* A_2 A_3 B_2	*h*0*l*$_o$ c A_2 A_3 B_2
	0*k*0 n A_3	00*l* 2$_{12}$ B_3	*h*00 2$_{11}$ B_3	00*l* 2$_{12}$ A_2 B_2 B_3	*h*00 2$_{11}$ A_2 B_2 B_3	
61 *P*2$_1$/*b*2$_1$/*c*2$_1$/*a*	00*l* c, 2$_{13}$ A_2 A_3 B_2 B_3	00*l* 2$_{13}$ B_3	0*k*0 *b*, 2$_{12}$ A_2 A_3 B_2 B_3	$h_o k0$ *a* A_2 A_3 B_2	0*k*$_o$*l* *b* A_2 A_3 B_2	*h*0*l*$_o$ c A_2 A_3 B_2
	0*k*0 2$_{12}$ B_3	*h*00 *a*, 2$_{11}$ A_2 A_3 B_2 B_3	*h*00 2$_{11}$ B_3	00*l* 2$_{13}$ A_2 B_2 B_3	*h*00 2$_{11}$ A_2 B_2 B_3	0*k*0 2$_{12}$ A_2 B_2 B_3
62 *P*2$_1$/*n*2$_1$/*m*2$_1$/*a*	00*l* 2$_{13}$ B_3 0*k*0 2$_{12}$	00*l* n, 2$_{13}$ A_2 A_3 B_2 B_3 *h*00 *a*, 2$_{11}$	0*k*0 n, 2$_{12}$ A_2 A_3 B_2 B_3	$h_o k0$ *a* A_2 A_3 B_2	0*kl*: $k + l =$ $2n + 1$ n A_2 A_3 B_2	0*k*0 2$_{12}$ A_2 B_2 B_3
			*h*00 2$_{11}$ B_3	00*l* 2$_{13}$ A_2 B_2 B_3	*h*00 2$_{11}$ A_2 B_2 B_3	
63 *C*2/*m*2/*c*2$_1$/*m*	00*l* c, 2$_1$ A_2 A_3 B_2 B_3	00*l* 2$_1$ B_3		00*l* 2$_1$ A_2 B_2 B_3		*h*$_e$0*l*$_o$ c A_2 A_3 B_2
64 *C*2/*m*2/*c*2$_1$/*a*	00*l* c, 2$_1$ A_2 A_3 B_2 B_3	00*l* 2$_1$ B_3		$h_o k_o 0$ *a* A_2 A_3 B_2		*h*$_e$0*l*$_o$ c A_2 A_3 B_2
				00*l* 2$_1$ A_2 B_2 B_3		
65 *C*2/*m*2/*m*2/*m*						
66 *C*2/*c*2/*c*2/*m*	00*l* c_2 A_3	00*l* c_1 A_3			0*k*$_e$*l*$_o$ c_1 A_2 A_3 B_2	*h*$_e$0*l*$_o$ c_2 A_2 A_3 B_2
67 *C*2/*m*2/*m*2/*a*				$h_o k_o 0$ *a* A_2 A_3 B_2		

Table 2.5.3.9 (*cont.*)

Space group	Incident-beam direction					
	[100]	[010]	[001]	[*hk*0]	[0*kl*]	[*h*0*l*]
68 *C*2/*c*2/*c*2/*a*	00*l* c_2 A_3	00*l* c_1 A_3		$h_o k_o 0$ A_2 B_2 *a* A_3	$0k_e l_o$ A_2 B_2 c_1 A_3	$h_e 0 l_o$ A_2 B_2 c_2 A_3
69 *F*2/*m*2/*m*2/*m*						
70 *F*2/*d*2/*d*2/*d*	00*l*: $l =$ A_3 $4n + 2$ d_2 0*k*0: $k =$ $4n + 2$ d_3	*h*00: $h =$ A_3 $4n + 2$ d_3 00*l*: $l =$ $4n + 2$ d_1	0*k*0: $k =$ A_3 $4n + 2$ d_1 *h*00: $h =$ $4n + 2$ d_2	$h_e k_e 0$: A_2 B_2 $h_e + k_e =$ A_3 $4n + 2$ d_3	$0k_e l_e$: A_2 B_2 $k_e + l_e =$ A_3 $4n + 2$ d_1	$h_e 0 l_e$: A_2 B_2 $h_e + l_e =$ A_3 $4n + 2$ d_2
71 *I*2/*m*2/*m*2/*m*						
72 *I*2/*b*2/*a*2/*m*					$0k_o l_o$ A_2 B_2 *b* A_3	$h_o 0 l_o$ A_2 B_2 *a* A_3
73 $I2_1/b2_1/c2_1/a$				$h_o k_o 0$ A_2 B_2 *a* A_3	$0k_o l_o$ A_2 B_2 *b* A_3	$h_o 0 l_o$ A_2 B_2 *c* A_3
74 $I2_1/m2_1/m2_1/a$				$h_o k_o 0$ A_2 B_2 *a* A_3		

Point groups 4, $\bar{4}$, 4/*m*

Space group	Incident-beam direction
	[*hk*0]
75 *P*4	
76 $P4_1$	00*l* A_2 B_2 4_1 B_3
77 $P4_2$	
78 $P4_3$	00*l* A_2 B_2 4_3 B_3
79 *I*4	
80 $I4_1$	
81 $P\bar{4}$	
82 $I\bar{4}$	
83 *P*4/*m*	
84 $P4_2/m$	
85 *P*4/*n*	*hk*0: $h + k = 2n + 1$ A_2 B_2 *n* A_3
86 $P4_2/n$	*hk*0: $h + k = 2n + 1$ A_2 B_2 *n* A_3
87 *I*4/*m*	
88 $I4_1/a$	$h_o k_o 0$ A_2 B_2 *a* A_3

Point group 422

Space group	Incident-beam direction	
	[*hk*0]	[0*kl*]
89 *P*422		
90 $P42_12$		*h*00 A_2 B_2 2_1 B_3
91 $P4_122$	00*l* A_2 B_2 4_1 B_3	
92 $P4_12_12$	00*l* A_2 B_2 4_1 B_3	*h*00 A_2 B_2 2_1 B_3
93 $P4_222$		
94 $P4_22_12$		*h*00 A_2 B_2 2_1 B_3
95 $P4_322$	00*l* A_2 B_2 4_3 B_3	
96 $P4_32_12$	00*l* A_2 B_2 4_3 B_3	*h*00 A_2 B_2 2_1 B_3
97 *I*422		
98 $I4_122$		

Table 2.5.3.9 (*cont.*)

Point group 4*mm*. The symbol *a* in the column [*h*0*l*] is equivalent to the symbol *b* in the space groups of the first column.

Space group		Incident-beam direction									
		[100]		[001]		[110]		[*h*0*l*]		[*hhl*]	
99	*P*4*mm*										
100	*P*4*bm*			*h*00 a_2 0*k*0 b_1	A_2 B_2 A_3			h_o0l *a*	A_2 B_2 A_3		
101	$P4_2cm$	00*l* c_2 A_3						*h*0l_o *c*	A_2 B_2 A_3		
102	$P4_2nm$	00*l* n_2 A_3		*h*00 n_2 0*k*0 n_1	A_2 B_2 A_3			*h*0*l*: $h + l = 2n + 1$ *n*	A_2 B_2 A_3		
103	*P*4*cc*	00*l* c_{12} A_3				00*l* c_2 A_3		*h*0l_o c_1	A_2 B_2 A_3	*hhl*$_o$ c_2	A_2 B_2 A_3
104	*P*4*nc*	00*l* n_2 A_3		*h*00 n_2 0*k*0 n_1	A_2 B_2 A_3	00*l* *c* A_3		*h*0*l*: $h + l = 2n + 1$ *n*	A_2 B_2 A_3	*hhl*$_o$ *c*	A_2 B_2 A_3
105	$P4_2mc$					00*l* *c* A_3				*hhl*$_o$ *c*	A_2 B_2 A_3
106	$P4_2bc$			*h*00 a_2 0*k*0 b_1	A_2 B_2 A_3	00*l* *c* A_3		h_o0l *a*	A_2 B_2 A_3	*hhl*$_o$ *c*	A_2 B_2 A_3
107	*I*4*mm*										
108	*I*4*cm*							h_o0l_o *c*	A_2 B_2 A_3		
109	$I4_1md$			*hh*0, $\bar{h}h0$ *d*	A_2 B_2 A_3	00*l*: $l = 4n + 2$ *d* A_3				*hhl*$_e$: $2h + l_e = 4n + 2$ *d*	A_2 B_2 A_3
110	$I4_1cd$			*hh*0, $\bar{h}h0$ *d*	A_2 B_2 A_3	00*l*: $l = 4n + 2$ *d* A_3		h_o0l_o *c*	A_2 B_2 A_3	*hhl*$_e$: $2h + l_e = 4n + 2$ *d*	A_2 B_2 A_3

Point group $\bar{4}2m$. The symbol *a* in the column [*h*0*l*] is equivalent to the symbol *b* in the space groups of the first column.

Space group		Incident-beam direction									
		[100]		[001]		[110]		[*h*0*l*]		[*hhl*]	
111	$P\bar{4}2m$										
112	$P\bar{4}2c$					00*l* *c* A_3				*hhl*$_o$ *c*	A_2 B_2 A_3
113	$P\bar{4}2_1m$	0*k*0 A_2 B_2 2_{12} B_3		*h*00 2_{11} 0*k*0 2_{12}	A_2 B_2 B_3			0*k*0 2_1	A_2 B_2 B_3		
114	$P\bar{4}2_1c$	0*k*0 A_2 B_2 2_{12} B_3		*h*00 2_{11} 0*k*0 2_{12}	A_2 B_2 B_3	00*l* *c* A_3		0*k*0 2_1	A_2 B_2 B_3	*hhl*$_o$ *c*	A_2 B_2 A_3
115	$P\bar{4}m2$										
116	$P\bar{4}c2$	00*l* c_2 A_3						*h*0l_o *c*	A_2 B_2 A_3		
117	$P\bar{4}b2$			*h*00 a_2 0*k*0 b_1	A_2 B_2 A_3			h_o0l *a*	A_2 B_2 A_3		
118	$P\bar{4}n2$	00*l* n_2 A_3		*h*00 n_2 0*k*0 n_1	A_2 B_2 A_3			*h*0*l*: $h + l = 2n + 1$ *n*	A_2 B_2 A_3		
119	$I\bar{4}m2$										
120	$I\bar{4}c2$							h_o0l_o *c*	A_2 B_2 A_3		
121	$I\bar{4}2m$										
122	$I\bar{4}2d$			*hh*0, $\bar{h}h0$ *d*	A_2 B_2 A_3	00*l*: $l = 4n + 2$ *d* A_3				*hhl*$_e$: $2h + l_e = 4n + 2$ *d*	A_2 B_2 A_3

Table 2.5.3.9 (*cont.*)

Point group 4/*mmm*. The symbol *a* in the column [*h*0*l*] is equivalent to the symbol *b* in the space groups of the first column.

Space group		Incident-beam direction					
		[100]	[001]	[110]	[*h*0*l*]	[*hhl*]	[*hk*0]
123	*P*4/*mmm* *P*4/*m*2/*m*2/*m*						
124	*P*4/*mcc* *P*4/*m*2/*c*2/*c*	00*l* c_{12} A_3		00*l* c_2 A_3	*h*0l_o A_2 B_2 c_1 A_3	*hhl*$_o$ A_2 B_2 c_2 A_3	
125	*P*4/*nbm* *P*4/*n*2/*b*2/*m*	0*k*0 *n* A_3	*h*00 a_2 A_3 0*k*0 b_1		h_o0*l* *a* A_2 B_2 A_3		*hk*0: A_2 B_2 *h* + *k* = 2*n* + 1 A_3 *n*
126	*P*4/*nnc* *P*4/*n*2/*n*2/*c*	0*k*0 n_1 A_3 00*l* n_{22}	*h*00 n_{22} A_3 0*k*0 n_{21}	00*l* *c* A_3	*h*0*l*: A_2 B_2 *h* + *l* = 2*n* + 1 A_3 n_2	*hhl*$_o$ A_2 B_2 *c* A_3	*hk*0: A_2 B_2 *h* + *k* = 2*n* + 1 A_3 n_1
127	*P*4/*mbm* *P*4/*m*2$_1$/*b*2/*m*	0*k*0 2_{12} B_3	*h*00 A_2 B_2 a_2, 2_{11} A_3 B_3 0*k*0 b_1, 2_{12}		*h*$_o$0*l* A_2 B_2 *a* A_3 0*k*0 A_2 B_2 2_1 B_3		
128	*P*4/*mnc* *P*4/*m*2$_1$/*n*2/*c*	00*l* n_2 A_3 0*k*0 2_{12} B_3	*h*00 A_2 B_2 n_2, 2_{11} A_3 B_3 0*k*0 n_1, 2_{12}	00*l* *c* A_3	*h*0*l*: A_2 B_2 *h* + *l* = 2*n* + 1 A_3 *n* 0*k*0 A_2 B_2 2_1 B_3	*hhl*$_o$ A_2 B_2 *c* A_3	
129	*P*4/*nmm* *P*4/*n*2$_1$/*m*2/*m*	0*k*0 A_2 B_2 *n*, 2_{12} A_3 B_3	*h*00 2_{11} B_3 0*k*0 2_{12}		0*k*0 A_2 B_2 2_1 B_3		*hk*0: A_2 B_2 *h* + *k* = 2*n* + 1 A_3 *n*
130	*P*4/*ncc* *P*4/*n*2$_1$/*c*2/*c*	0*k*0 A_2 B_2 *n*, 2_{12} A_3 B_3 00*l* c_{12} A_3	*h*00 2_{11} B_3 0*k*0 2_{12}	00*l* c_2 A_3	*h*0l_o A_2 B_2 c_1 A_3 0*k*0 A_2 B_2 2_1 B_3	*hhl*$_o$ A_2 B_2 c_2 A_3	*hk*0: A_2 B_2 *h* + *k* = 2*n* + 1 A_3 *n*
131	*P*4$_2$/*mmc* *P*4$_2$/*m*2/*m*2/*c*			00*l* *c* A_3		*hhl*$_o$ A_2 B_2 *c* A_3	
132	*P*4$_2$/*mcm* *P*4$_2$/*m*2/*c*2/*m*	00*l* c_2 A_3			*h*0l_o A_2 B_2 *c* A_3		
133	*P*4$_2$/*nbc* *P*4$_2$/*n*2/*b*2/*c*	0*k*0 *n* A_3	*h*00 a_2 A_3 0*k*0 b_1	00*l* *c* A_3	h_o0*l* *a* A_2 B_2 A_3	*hhl*$_o$ A_2 B_2 *c* A_3	*hk*0: A_2 B_2 *h* + *k* = 2*n* + 1 A_3 *n*
134	*P*4$_2$/*nnm* *P*4$_2$/*n*2/*n*2/*m*	0*k*0 n_1 A_3 00*l* n_{22}	*h*00 n_{22} A_3 0*k*0 n_{21}		*h*0*l*: A_2 B_2 *h* + *l* = 2*n* + 1 A_3 n_2		*hk*0: A_2 B_2 *h* + *k* = 2*n* + 1 A_3 n_1
135	*P*4$_2$/*mbc* *P*4$_2$/*m*2$_1$/*b*2/*c*	0*k*0 2_{12} B_3	*h*00 A_2 B_2 a_2, 2_{11} A_3 B_3 0*k*0 b_1, 2_{12}	00*l* *c* A_3	*h*$_o$0*l* A_2 B_2 *a* A_3 0*k*0 A_2 B_2 2_1 B_3	*hhl*$_o$ A_2 B_2 *c* A_3	
136	*P*4$_2$/*mnm* *P*4$_2$/*m*2$_1$/*n*2/*m*	00*l* n_2 A_3 0*k*0 2_{12} B_3	*h*00 A_2 B_2 n_2, 2_{11} A_3 B_3 0*k*0 n_1, 2_{12}		*h*0*l*: A_2 B_2 *h* + *l* = 2*n* + 1 A_3 *n* 0*k*0 A_2 B_2 2_1 B_3		
137	*P*4$_2$/*nmc* *P*4$_2$/*n*2$_1$/*m*2/*c*	0*k*0 A_2 B_2 *n*, 2_{12} A_3 B_3	*h*00 2_{11} B_3 0*k*0 2_{12}	00*l* *c* A_3	0*k*0 A_2 B_2 2_1 B_3	*hhl*$_o$ A_2 B_2 *c* A_3	*hk*0: A_2 B_2 *h* + *k* = 2*n* + 1 A_3 *n*
138	*P*4$_2$/*ncm* *P*4$_2$/*n*2$_1$/*c*2/*m*	0*k*0 A_2 B_2 *n*, 2_{12} A_3 B_3 00*l* c_2 A_3	*h*00 2_{11} B_3 0*k*0 2_{12}		*h*0l_o A_2 B_2 *c* A_3 0*k*0 A_2 B_2 2_1 B_3		*hk*0: A_2 B_2 *h* + *k* = 2*n* + 1 A_3 *n*
139	*I*4/*mmm* *I*4/*m*2/*m*2/*m*						

Table 2.5.3.9 (*cont.*)

Space group	Incident-beam direction					
	[100]	[001]	[110]	[*h*0*l*]	[*hhl*]	[*hk*0]
140 *I*4/*mcm* *I*4/*m*2/*c*2/*m*				h_o0l_o A_2 B_2 *c* A_3		
141 $I4_1/amd$ $I4_1/a2/m2/d$		*hh*0, $\bar{h}h0$ *d* A_3	00*l*: *l* = A_3 4*n* + 2 *d* $\bar{h}h0$ *a*		*hhl*$_e$: A_2 B_2 2*h* + l_e = A_3 4*n* + 2 *d*	h_ok0 A_2 B_2 *a* A_3
142 $I4_1/acd$ $I4_1/a2/c2/d$		*hh*0, $\bar{h}h0$ *d* A_3	00*l*: *l* = A_3 4*n* + 2 *d* $\bar{h}h0$ *a*	h_o0l_o A_2 B_2 *c* A_3	*hhl*$_e$: A_2 B_2 2*h* + l_e = A_3 4*n* + 2 *d*	h_ok0 A_2 B_2 *a* A_3

Point groups 3, $\bar{3}$, 32, 3*m*, $\bar{3}m$

Space group	Incident-beam direction	
	[11$\bar{2}$0]	[1$\bar{1}$00]
Nos. 143–155: no GM line		
156 *P*3*m*1		
157 *P*31*m*		
158 *P*3*c*1		00*l* A_2 B_2 *c* A_3
159 *P*31*c*	00*l* A_2 B_2 *c* A_3	
160 *R*3*m*		
161 *R*3*c*		00*l*: *l* = 6*n* + 3 A_2 B_2 *c* A_3
162 $P\bar{3}1m$		
163 $P\bar{3}1c$	00*l* A_2 B_2 *c* A_3	
164 $P\bar{3}m1$		
165 $P\bar{3}c1$		00*l* A_2 B_2 *c* A_3
166 $R\bar{3}m$		
167 $R\bar{3}c$		00*l*: *l* = 6*n* + 3 A_2 B_2 *c* A_3

Point groups 6, $\bar{6}$, 6/*m*, 622, 6*mm*, $\bar{6}m2$, 6/*mmm*

Space group	Incident-beam direction	
	[11$\bar{2}$0]	[1$\bar{1}$00]
168 *P*6		
169 $P6_1$	00*l* A_2 B_2 6_1 B_3	00*l* A_2 B_2 6_1 B_3
170 $P6_5$	00*l* A_2 B_2 6_5 B_3	00*l* A_2 B_2 6_5 B_3
171 $P6_2$		
172 $P6_4$		
173 $P6_3$	00*l* A_2 B_2 6_3 B_3	00*l* A_2 B_2 6_3 B_3
174 $P\bar{6}$		
175 *P*6/*m*		
176 $P6_3/m$	00*l* A_2 B_2 6_3 B_3	00*l* A_2 B_2 6_3 B_3

Table 2.5.3.9 (*cont.*)

Space group		Incident-beam direction					
		[11$\bar{2}$0]			[1$\bar{1}$00]		
177	$P622$						
178	$P6_122$	$00l$ 6_1	A_2	B_2 B_3	$00l$ 6_1	A_2	B_2 B_3
179	$P6_522$	$00l$ 6_5	A_2	B_2 B_3	$00l$ 6_5	A_2	B_2 B_3
180	$P6_222$						
181	$P6_422$						
182	$P6_322$	$00l$ 6_3	A_2	B_2 B_3	$00l$ 6_3	A_2	B_2 B_3
183	$P6mm$						
184	$P6cc$	$00l$ c_2	A_3		$00l$ c_1	A_3	
185	$P6_3cm$	$00l$ 6_3		B_3	$00l$ 6_3, c	A_2 A_3	B_2 B_3
186	$P6_3mc$	$00l$ 6_3, c	A_2 A_3	B_2 B_3	$00l$ 6_3		B_3
187	$P\bar{6}m2$						
188	$P\bar{6}c2$				$00l$ c	A_2 A_3	B_2
189	$P\bar{6}2m$						
190	$P\bar{6}2c$	$00l$ c	A_2 A_3	B_2			
191	$P6/mmm$						
192	$P6/mcc$	$00l$ c_2	A_3		$00l$ c_1	A_3	
193	$P6_3/mcm$	$00l$ 6_3		B_3	$00l$ 6_3, c	A_2 A_3	B_2 B_3
194	$P6_3/mmc$	$00l$ 6_3, c	A_2 A_3	B_2 B_3	$00l$ 6_3		B_3

Point groups 23, $m3$

Space group		Incident-beam direction							
		[100] (cyclic)			[110] (cyclic)			[hk0] (cyclic)		
195	$P23$								
196	$F23$								
197	$I23$								
198	$P2_13$	$00l$ 2_{13} $0k0$ 2_{12}	A_2	B_2 B_3	$00l$ 2_{13}	A_2	B_2 B_3	$00l$ 2_1	A_2	B_2 B_3
199	$I2_13$								
200	$Pm3$ $P2/m\bar{3}$								
201	$Pn3$ $P2/n\bar{3}$	$00l$ n_2 $0k0$ n_3	A_3					$\bar{k}h0$ n	A_2 A_3	B_2
202	$Fm3$ $F2/m\bar{3}$									
203	$Fd3$ $F2/d\bar{3}$	$00l$: $l = 4n + 2$ d_2 $0k0$: $k = 4n + 2$ d_3	A_3					$\bar{k}h0$: $h + k = 4n + 2$ d	A_2 A_3	B_2
204	$Im3$ $I2/m\bar{3}$									
205	$Pa3$ $P2_1/a\bar{3}$	$00l$ c_2, 2_{13}	A_2 A_3	B_2 B_3	$00l$ 2_{13}	A_2	B_2 B_3	$00l$ 2_1	A_2	B_2 B_3
		$0k0$ 2_{12}		B_3	$\bar{h}h0$ a_3	A_2 A_3	B_2	$\bar{k}h0$ a	A_2 A_3	B_2
206	$Ia3$ $I2_1/a\bar{3}$				$\bar{h}h0$ a_3	A_2 A_3	B_2	$\bar{k}h0$ a	A_2 A_3	B_2

Table 2.5.3.9 (*cont.*)

Point group 432

Space group		Incident-beam direction [*hk*0] (cyclic)		
207	$P432$			
208	$P4_232$			
209	$F432$			
210	$F4_132$			
211	$I432$			
212	$P4_332$	$00l$ 4_3	A_2	B_2 B_3
213	$P4_132$	$00l$ 4_1	A_2	B_2 B_3
214	$I4_132$			

Point group $\bar{4}3m$

Space group		Incident-beam direction [100] (cyclic)		[110] (cyclic)		[*hhl*] (cyclic)		
215	$P\bar{4}3m$							
216	$F\bar{4}3m$							
217	$I\bar{4}3m$							
218	$P\bar{4}3n$			$00l$ n	 A_3	hhl_o n	A_2 A_3	B_2
219	$F\bar{4}3c$					$h_oh_ol_o$ c	A_2 A_3	B_2
220	$I\bar{4}3d$	$0kk$, $0\bar{k}k$ d	A_2 A_3	$00l$: $l = 4n + 2$ d	 A_3	hhl_e: $2h + l_e = 4n + 2$ d	A_2 A_3	B_2

Point group $m3m$

Space group		Incident-beam direction [100] (cyclic)		[110] (cyclic)		[*hk*0] (cyclic)			[*hhl*] (cyclic)		
221	$Pm3m$ $P4/m\bar{3}2/m$										
222	$Pn3n$ $P4/n\bar{3}2/n$	$00l$ n_{12} $0k0$ n_{13}	 A_3	$00l$ n_2	 A_3	$hk0$: $h + k = 2n + 1$ n_1	A_2 A_3	B_2	hhl_o n_2	A_2 A_3	B_2
223	$Pm3n$ $P4_2/m\bar{3}2/n$			$00l$ n	 A_3				hhl_o n	A_2 A_3	B_2
224	$Pn3m$ $P4_2/n\bar{3}2/m$	$00l$ n_2 $0k0$ n_3	 A_3			$hk0$: $h + k = 2n + 1$ n	A_2 A_3	B_2			
225	$Fm3m$ $F4/m\bar{3}2/m$										
226	$Fm3c$ $F4/m\bar{3}2/c$								$h_oh_ol_o$ c	A_2 A_3	B_2
227	$Fd3m$ $F4_1/d\bar{3}2/m$	$00l$: $l = 4n + 2$ d_2 $0k0$: $k = 4n + 2$ d_3	 A_3			h_ek_e0: $h_e + k_e = 4n + 2$ d	A_2 A_3	B_2			
228	$Fd3c$ $F4_1/d\bar{3}2/c$	$00l$: $l = 4n + 2$ d_2 $0k0$: $k = 4n + 2$ d_3	 A_3			h_ek_e0: $h_e + k_e = 4n + 2$ d	A_2 A_3	B_2	$h_oh_ol_o$ c	A_2 A_3	B_2
229	$Im3m$ $I4/m\bar{3}2/m$										
230	$Ia3d$ $I4_1/a\bar{3}2/d$	$0kk$, $0\bar{k}k$ d	 A_3	$00l$: $l = 4n + 2$ d $\bar{h}h0$ a_3	 A_3	h_ok_o0 a	A_2 A_3	B_2	hhl_e: $2h + l_e = 4n + 2$ d	A_2 A_3	B_2

Table 2.5.3.10. *Space-group sets indistinguishable by dynamical extinction lines*

(1) $P3$, ($P3_1$, $P3_2$)	(2) $P312$, ($P3_112$, $P3_212$)	(3) $P321$, ($P3_121$, $P3_221$)
(4) $P6$, ($P6_2$, $P6_4$)	(5) $P622$, ($P6_222$, $P6_422$)	(6) $P6_3$, ($P6_1$, $P6_5$)
(7) $P6_322$, ($P6_122$, $P6_522$)	(8) $P4$, $P4_2$	(9) ($P4_1$, $P4_3$)
(10) $P4/m$, $P4_2/m$	(11) $P4/n$, $P4_2/n$	(12) $P422$, $P4_222$
(13) $P42_12$, $P4_22_12$	(14) $I4$, $I4_1$	(15) $I422$, $I4_122$
(16) $I23$, $I2_13$	(17) $I222$, $I2_12_12_1$	(18) $P432$, $P4_232$
(19) ($P4_132$, $P4_332$)	(20) $I432$, $I4_132$	(21) $F432$, $F4_132$
(22) ($P4_122$, $P4_322$)	(23) ($P4_12_12$, $P4_32_12$)	

distinguishes the difference in the relative arrangements of twofold rotation axes and 2_1 screw axes along the [111] direction between the two space groups by examining the symmetry of intensity pairs appearing in the overlapping discs of a coherent [111] ZOLZ pattern. Saitoh, Tsuda *et al.* (2001) extended the method to distinguish the other ten indistinguishable space-group pairs. The method can distinguish between a space group which is composed of a principal rotation axis and a twofold rotation axis like $P321$ and a space group which is composed of a principal screw axis and a twofold rotation axis like $P3_121$ (or $P3_221$) by investigating the difference in the relative arrangements of the twofold rotation axis with respect to the principal axis. Table 2.5.3.11 shows the 12 space-group pairs which are distinguishable by applying the coherent CBED method.

The pairs in parentheses form left- and right-handed space groups. Handedness or chirality may occur in space groups that do not possess mirror and/or inversion symmetry. The handedness of space groups is identified in such a way that the senses of two crystal axes are determined with the aid of kinematical structure-factor calculations and the sense of the third axis is determined with the aid of dynamical calculations. This method was used for quartz by Goodman & Secomb (1977) and Goodman & Johnson (1977) and for MnSi by Tanaka *et al.* (1985). We also mention that Taftø & Spence (1982) developed a simple but clever method without computation for determining the absolute polarity of the sphalerite structure utilizing multiple-scattering effects on weak beams, which are almost independent of thickness. Because of the importance of structure in the field of semiconductor science, this method is conveniently used nowadays to determine polarity.

It is worth mentioning that space groups that are indistinguishable by CBED (Table 2.5.3.10) do not appear frequently in real inorganic materials. The crystal data collected by Nowacki (1967) on 5572 different inorganic materials shows that the number of materials belonging to space groups among sets (2), (3), (5), (7) and (11) in Table 2.5.3.10 is more than 15 but the number belonging to space groups among the other sets is less than ten. This implies that the probability of finding indistinguishable space groups is very low.

Table 2.5.3.11. *Space-group sets distinguishable by coherent CBED*

The space-group pairs in parentheses can not be distinguished by coherent CBED but can be distinguished by a handedness test. An asterisk (*) indicates the incidence at which the distinction is carried out by many-beam interference (Saitoh, Tsuda *et al.*, 2001).

Space-group set	Incidence
(2) $P312$, ($P3_112$, $P3_212$)	$[1\bar{1}01]$
(3) $P321$, ($P3_121$, $P3_221$)	$[11\bar{2}3]$
(5) $P622$, ($P6_222$, $P6_422$)	$[11\bar{2}3]$
(7) $P6_322$, ($P6_122$, $P6_522$)	$[11\bar{2}3]$
(12) $P422$, $P4_222$	[321], [211], [112]*
(13) $P42_12$, $P4_22_12$	[211]
(15) $I422$, $I4_122$	[111]
(16) $I23$, $I2_13$	[111]
(17) $I222$, $I2_12_12_1$	[111]
(18) $P432$, $P4_232$	[321], [211]*
(20) $I432$, $I4_132$	[111]
(21) $F432$, $F4_132$	[432]

2.5.3.3.4. Dynamical extinction in HOLZ reflections

Space-group determination as described in the previous sections is carried out using the extinction lines appearing in ZOLZ reflections. Vertical glide planes whose translation vectors are perpendicular to the specimen surface do not cause extinction lines in ZOLZ reflections but cause them in HOLZ reflections. (It is noted that the vertical glide planes with glide translations not parallel to the surface are not the symmetry elements of diperiodic plane figures.) Vertical glide planes whose translation vectors are parallel to the surface cause extinction lines in both ZOLZ and HOLZ reflections. Vertical screw axes are expected to form extinction lines in HOLZ reflections whose vectors are parallel to the screw axes. These reflections, however, cannot be observed by ordinary CBED. Thus, the extinction lines appearing in observable HOLZ reflections are used to identify not screw axes but glide planes. Examination of HOLZ extinction lines together with ZOLZ extinction lines is an efficient way to characterize the glide vectors and determine the space group.

The dynamical extinction lines appearing in HOLZ reflections caused by the glide planes whose glide vectors are not only parallel but also not parallel to the specimen surface were tabulated by Nagasawa (1983) for various incident-beam orientations of all the space groups that have glide planes. The tabulated results appear on pages 214–225 of the book by Tanaka *et al.* (1988). Table 2.5.3.12 shows the results. The meanings of the letters used in the table are explained in Fig. 2.5.3.13. We consider a vertical glide plane with a glide vector perpendicular to the surface as is shown in Fig. 2.5.3.13(*a*). Letter *A* is given for cases in which the Ewald sphere intersects two circled-cross reflections in the first Laue zone as seen in Fig. 2.5.3.13(*b*), where black circles and circled crosses denote allowed reflections and kinematically forbidden but dynamically allowed reflections due to the glide plane, respectively. *A** denotes cases in which the Ewald sphere intersects a circled-cross reflection on one side of the incident beam and a black-circled reflection on the other, as seen in Fig. 2.5.3.13(*c*). This case occurs only in space group $P2_1/a\bar{3}$. A_h denotes cases in which the Ewald sphere intersects a circled-cross reflection on one side but does not intersect on the other, owing to the asymmetric arrangement of reflections with respect to the incident beam.

The first column of Table 2.5.3.12 list the space groups and the following columns show the type of the extinction lines for possible incident-beam directions. In each pair of columns, the left-hand column gives the reflection indices of the extinction line and the symmetry elements causing the extinction and the right-hand column gives the type of extinction. The first suffix 1, 2 or 3 of a glide symbol distinguishes the first, the second or the third glide plane of a space group. The second suffixes 1 and 2, which appear in the tetragonal and cubic systems, distinguish two equivalent glide planes which lie in the *x* and *y* planes. The suffix o of a reflection index implies that the index is odd-order. Figs.

2.5.3.14(*a*) and (*b*) were taken for FeS_2, space group $P2_1/a\bar{3}$, with incident-beam directions of [100] and [110]. Inserts show enlarged HOLZ patterns for ease of viewing. Extinction lines of type *A* are seen in the $h_o k0$ HOLZ reflections in Fig. 2.5.3.14(*a*) due to the *b*-glide plane (equivalent to the *a*-glide plane in the space-group symbol) parallel to the (001) plane. An extinction line *A** is seen in an $h_o k0$ HOLZ reflection in Fig. 2.5.3.14(*b*) due to the same glide plane as that of Fig. 2.5.3.14(*a*). It should be noted that extinction lines in HOLZ reflections are better observed in thinner specimen areas than those suitable for the observation of the extinction lines in ZOLZ reflections, because the profiles of HOLZ reflections are concentrated into small areas of CBED discs in thicker specimens.

In summary, the use of not only ZOLZ, but also HOLZ extinction lines is recommended for space-group determination.

2.5.3.3.5. Symmetry elements observed by CBED

In the above sections, point-group and space-group determination methods were described following the theory of Buxton *et al.* (1976). They assumed that the observable symmetry elements are those of an infinitely extended parallel-sided specimen or of diperiodic plane figures. CBED patterns determine diffraction groups. Crystal point groups are identified by consulting Fig. 2.5.3.4, which gives the relations between diffraction groups and crystal point groups. When the assumption made by Buxton *et al.* (1976) is accepted in a strict sense, CBED symmetry m_2 caused by a twofold rotation axis oblique to the specimen surface, which is not a symmetry element of a diperiodic plane figure, ought not to be observed. However, the symmetry m_2 due to a twofold rotation axis in the $[1\bar{1}0]$ direction of an Si film with [100] surface normal has been clearly observed at [111] electron incidence (Tanaka *et al.*, 1988, p. 33). This indicates that crystal symmetry elements oblique to the specimen surface are observable when the specimen is tilted. An important condition for CBED is that the top and bottom surfaces be parallel over the specimen area illuminated by the incident beam. CBED observes the symmetry elements of a crystal to the extent that the boundary conditions at the specimen surface do not break the symmetries of the CBED patterns. Gjønnes & Gjønnes (1985) reported that the breaking of CBED symmetry due to a surface oblique to the incident beam is practically negligible.

In Section 2.5.3.3 on space-group determination, space-group symmetry elements of crystals which have glide and screw components parallel to the specimen surface were considered to act as space-group symmetry elements of diperiodic plane figures by mitigating the strict application of the assumption of diperiodic plane figures. In fact, vertical glide planes with a glide vector not parallel to the specimen surface, which were dealt in Section 2.5.3.3.4, are not the symmetry elements of diperiodic plane figures. Ishizuka (1982) showed theoretically that a vertical glide plane with a vertical glide vector produces dynamical extinction lines in HOLZ discs if the Laue zones are well separated. Tanaka *et al.* (1988, pp. 214–225) tabulated the extinction lines appearing in HOLZ discs caused by the vertical glide planes whose glide vectors are not only parallel but also not parallel to the specimen surface. Dynamical extinction lines caused by the glide planes with a glide vector not parallel to the surface have been demonstrated using FeS_2 and $MgAl_2O_4$ (Tanaka *et al.*, 1988, pp. 51–61).

Vertical 2_1, 3_1, 3_2, ..., 6_5 screw axes, which are not symmetry elements of diperiodic plane figures, are expected to form dynamical extinction lines in kinematically forbidden reflections that are located in the direction of the screw axes or of the surface normal. The extinction lines, however, are difficult to observe in ordinary CBED. Thus, CBED does not observe all the symmetry elements of the crystal space groups but observes many more symmetry elements than those of the diperiodic plane figures. It is clear now that it makes no sense to construct space groups using actually observable symmetry elements because they do not form a complete set of groups. It is of no importance to give the relation between the 230 space groups of crystals and the 80 space groups of diperiodic plane figures. Buxton *et al.*'s theory, which determines crystal point groups with the help of diperiodic plane figures, is very beautiful and successful. However, it is not correct to state that CBED observes the symmetry elements of the diperiodic plane figures. The use of the groups of diperiodic plane figures should be recognized as a convention for the sake of convenience. As a further example, horizontal screw axes and horizontal glide planes must be located at the middle of a specimen to form symmetry elements of the diperiodic plane figures. However, those screw axes and glide planes which are not located at the middle of a specimen do produce CBED symmetries. Since we now know that CBED does not observe the symmetries of the diperiodic plane figures but observes those of a physical crystalline specimen, we can determine the corresponding infinite crystal symmetries more freely, by using our knowledge of the symmetries of the sample concerned, guided but not restricted by the beautiful theory of Buxton *et al.* (1976).

One point to note, for symmetry determination, is that one has to be aware of spurious symmetries that appear for crystals of certain structure types (Tanaka *et al.*, 1988, pp. 20–32 and 42–45) and destroy the correct determination of the point and space groups. Another point for precise symmetry determination is that one has to be aware of how CBED symmetry is destroyed by a small breakdown of crystal symmetry (Tanaka *et al.*, 1988 pp. 46–47).

2.5.3.3.6. Examples of space-group determination

A simple example of point-group determination has already been given for Si in Section 2.5.3.2.5. In this section, two examples of space-group determination for rutile and samarium selenide are described, in which the point-group determination still accounts for an important part. The examples look to be a little sophisticated but are a good exercise for those who want to acquire experience in CBED space-group determination. The present determination is carried out by assuming the lattice parameters to be known.

Rutile (TiO_2). The space group of rutile is well known to be $P4_2/mnm$. The lattice parameters are $a = b = 0.459$ nm and $c = 0.296$ nm. Fig. 2.5.3.15(*a*) shows a CBED pattern taken with the [001] incidence at an accelerating voltage of 80 kV. Since no fine HOLZ lines appear in all the discs, projection diffraction groups (column VI of Table 2.5.3.3) have to be applied to explain this pattern. The projection (proj.) WP shows symmetry 4*mm*. The projection diffraction group is found to be $4mm1_R$ from Table 2.5.3.3. Thus, possible diffraction groups are $4m_Rm_R$, 4*mm*, 4_Rmm_R and $4mm1_R$. Another CBED pattern at a second crystal orientation needs to be taken because Fig. 2.5.3.15(*a*) shows only projection symmetry. Figs. 2.5.3.15(*b*) and (*c*) show CBED patterns taken with the [101] incidence at an accelerating voltage of 100 kV. In Fig. 2.5.3.15(*b*), which is the central part of Fig. 2.5.3.15(*c*), no HOLZ lines are seen. The symmetries of the projection BP and projection WP are both 2*mm*. The projection diffraction group of the pattern is $2mm1_R$. The WP of Fig. 2.5.3.15*(c)* is seen to have one mirror symmetry *m*. The diffraction groups which satisfy symmetry *m* are *m*, $m1_R$ and 2_Rmm_R. Among these diffraction groups, the diffraction group whose projection becomes $2mm1_R$ is only diffraction group 2_Rmm_R. By consulting Fig. 2.5.3.4, diffraction group 2_Rmm_R obtained from Figs. 2.5.3.15(*b*) and (*c*) and one diffraction group $4mm1_R$ among diffraction groups $4m_Rm_R$, 4*mm*, 4_Rmm_R and $4mm1_R$ obtained from Fig. 2.5.3.15(*a*) commonly satisfy point group 4/*mmm*. Thus, the point group of rutile is determined to be 4/*mmm*.

Fig. 2.5.3.15(*d*) shows an ordinary diffraction pattern taken with the [001] incidence at an accelerating voltage of 80 kV. With the help of the lattice parameters and the camera length, the indices of the reflections are given as shown in the figure. There

Table 2.5.3.12. *Dynamical extinction lines appearing in HOLZ reflections for crystal space groups that have mirror and glide planes*

Point groups m, $2/m$ (second setting, unique axis b)

Space group		Incident-beam direction [$u0w$]	
6	Pm		
7	Pc	$h0l_o$ c	A_h
8	Cm		
9	Cc	h_e0l_o c	A_h
10	$P2/m$		
11	$P2_1/m$		
12	$C2/m$		
13	$P2/c$	$h0l_o$ c	A_h
14	$P2_1/c$	$h0l_o$ c	A_h
15	$C2/c$	h_e0l_o c	A_h

Point group $mm2$

Space group		Incident-beam direction [100]		[010]		[001]		[$0vw$]		[$u0w$]	
25	$Pmm2$										
26	$Pmc2_1$	$h0l_o$ c	A			$h0l_o$ c	A			$h0l_o$ c	A_h
27	$Pcc2$	$h0l_o$ c_2	A	$0kl_o$ c_1	A	$0kl_o$ c_1 $h0l_o$ c_2	A	$0kl_o$ c_1	A_h	$h0l_o$ c_2	A_h
28	$Pma2$	h_o0l a	A			h_o0l a	A			h_o0l a	A_h
29	$Pca2_1$	h_o0l a	A	$0kl_o$ c	A	$0kl_o$ c h_o0l a	A	$0kl_o$ c	A_h	h_o0l a	A_h
30	$Pnc2$	$h0l_o$ c	A	$0kl$: $k + l = 2n + 1$ n	A	$0kl$: $k + l = 2n + 1$ n $h0l_o$ c	A	$0kl$: $k + l = 2n + 1$ n	A_h	$h0l_o$ c	A_h
31	$Pmn2_1$	$h0l$: $h + l = 2n + 1$ n	A			$h0l$: $h + l = 2n + 1$ n	A			$h0l$: $h + l = 2n + 1$ n	A_h
32	$Pba2$	h_o0l a	A	$0k_ol$ b	A	$0k_ol$ b h_o0l a	A	$0k_ol$ b	A_h	h_o0l a	A_h
33	$Pna2_1$	h_o0l a	A	$0kl$: $k + l = 2n + 1$ n	A	$0kl$: $k + l = 2n + 1$ n h_o0l a	A	$0kl$: $k + l = 2n + 1$ n	A_h	h_o0l a	A_h
34	$Pnn2$	$h0l$: $h + l = 2n + 1$ n_2	A	$0kl$: $k + l = 2n + 1$ n_1	A	$0kl$: $k + l = 2n + 1$ n_1 $h0l$: $h + l = 2n + 1$ n_2	A	$0kl$: $k + l = 2n + 1$ n_1	A_h	$h0l$: $h + l = 2n + 1$ n_2	A_h
35	$Cmm2$ $ba2$										
36	$Cmc2_1$ $bn2_1$	h_e0l_o c	A			h_e0l_o c	A			h_e0l_o c	A_h
37	$Ccc2$ $nn2$	h_e0l_o c_2	A	$0k_el_o$ c_1	A	$0k_el_o$ c_1 h_e0l_o c_2	A	$0k_el_o$ c_1	A_h	h_e0l_o c_2	A_h

Table 2.5.3.12 (*cont.*)

Space group		Incident-beam direction									
		[100]		[010]		[001]		[0*vw*]		[*u*0*w*]	
38	*Amm*2 *nc*2_1										
39	*Abm*2 *cc*2_1			$0k_ol_o$ *b*	*A*	$0k_ol_o$ *b*	*A*	$0k_ol_o$ *b*	A_h		
40	*Ama*2 *nn*2_1	h_o0l_e *a*	*A*			h_o0l_e *a*	*A*			h_o0l_e *a*	A_h
41	*Aba*2 *cn*2_1	h_o0l_e *a*	*A*	$0k_ol_o$ *b*	*A*	$0k_ol_o$ *b* h_o0l_e *a*	*A*	$0k_ol_o$ *b*	A_h	h_o0l_e *a*	A_h
42	*Fmm*2										
43	*Fdd*2 *dd*2_1	h_e0l_e: $h_e + l_e = 4n + 2$ d_2	*A*	$0k_el_e$: $k_e + l_e = 4n + 2$ d_1	*A*	$0k_el_e$: $k_e + l_e = 4n + 2$ d_1 h_e0l_e: $h_e + l_e = 4n + 2$ d_2	*A*	$0k_el_e$: $k_e + l_e = 4n + 2$ d_1	A_h	h_e0l_e: $h_e + l_e = 4n + 2$ d_2	A_h
44	*Imm*2 *nn*2_1										
45	*Iba*2 *cc*2_1	h_o0l_o *a*	*A*	$0k_ol_o$ *b*	*A*	$0k_ol_o$ *b* h_o0l_o *a*	*A*	$0k_ol_o$ *b*	A_h	h_o0l_o *a*	A_h
46	*Ima*2 *nc*2_1	h_o0l_o *a*	*A*			h_o0l_o *a*	*A*			h_o0l_o *a*	A_h

Point group *mmm*

Space group		Incident-beam direction											
		[100]		[010]		[001]		[*uv*0]		[0*vw*]		[*u*0*w*]	
47	*P*2/*m*2/*m*2/*m*												
48	*P*2/*n*2/*n*2/*n*	*h*0*l*: $h + l = 2n + 1$ n_2 *hk*0: $h + k = 2n + 1$ n_3	*A*	0*kl*: $k + l = 2n + 1$ n_1 *hk*0: $h + k = 2n + 1$ n_3	*A*	0*kl*: $k + l = 2n + 1$ n_1 *h*0*l*: $h + l = 2n + 1$ n_2	*A*	*hk*0: $h + k = 2n + 1$ n_3	A_h	0*kl*: $k + l = 2n + 1$ n_1	A_h	*h*0*l*: $h + l = 2n + 1$ n_2	A_h
49	*P*2/*c*2/*c*2/*m*	$h0l_o$ c_2	*A*	$0kl_o$ c_1	*A*	$0kl_o$ c_1 $h0l_o$ c_2	*A*			$0kl_o$ c_1	A_h	$h0l_o$ c_2	A_h
50	*P*2/*b*2/*a*2/*n*	h_o0l *a* *hk*0: $h + k = 2n + 1$ *n*	*A*	$0k_ol$ *b* *hk*0: $h + k = 2n + 1$ *n*	*A*	$0k_ol$ *b* h_o0l *a*	*A*	*hk*0: $h + k = 2n + 1$ *n*	A_h	$0k_ol$ *b*	A_h	h_o0l *a*	A_h
51	$P2_1$/*m*2/*m*2/*a*	h_ok0 *a*	*A*	h_ok0 *a*	*A*			h_ok0 *a*	A_h				
52	*P*2/*n*2_1/*n*2/*a*	*h*0*l*: $h + l = 2n + 1$ n_2 h_ok0 *a*	*A*	0*kl*: $k + l = 2n + 1$ n_1 h_ok0 *a*	*A*	0*kl*: $k + l = 2n + 1$ n_1 *h*0*l*: $h + l = 2n + 1$ n_2	*A*	h_ok0 *a*	A_h	0*kl*: $k + l = 2n + 1$ n_1	A_h	*h*0*l*: $h + l = 2n + 1$ n_2	A_h
53	*P*2/*m*2/*n*2_1/*a*	*h*0*l*: $h + l = 2n + 1$ *n* h_ok0 *a*	*A*	h_ok0 *a*	*A*	*h*0*l*: $h + l = 2n + 1$ *n*	*A*	h_ok0 *a*	A_h			*h*0*l*: $h + l = 2n + 1$ *n*	A_h
54	$P2_1$/*c*2/*c*2/*a*	$h0l_o$ c_2 h_ok0 *a*	*A*	$0kl_o$ c_1 h_ok0 *a*	*A*	$0kl_o$ c_1 $h0l_o$ c_2	*A*	h_ok0 *a*	A_h	$0kl_o$ c_1	A_h	$h0l_o$ c_2	A_h

Table 2.5.3.12 (*cont.*)

Space group		Incident-beam direction											
		[100]		[010]		[001]		[uv0]		[0vw]		[u0w]	
55	$P2_1/b2_1/a2/m$	h_o0l a	A	$0k_ol$ b	A	$0k_ol$ b h_o0l a	A			$0k_ol$ b	A_h	h_o0l a	A_h
56	$P2_1/c2_1/c2/n$	$h0l_o$ c_2 $hk0$: $h + k =$ $2n + 1$ n	A	$0kl_o$ c_1 $hk0$: $h + k =$ $2n + 1$ n	A	$0kl_o$ c_1 $h0l_o$ c_2	A	$hk0$: $h + k =$ $2n + 1$ n	A_h	$0kl_o$ c_1	A_h	$h0l_o$ c_2	A_h
57	$P2/b2_1/c2_1/m$	$h0l_o$ c	A	$0k_ol$ b	A	$0k_ol$ b $h0l_o$ c	A			$0k_ol$ b	A_h	$h0l_o$ c	A_h
58	$P2_1/n2_1/n2/m$	$h0l$: $h + l =$ $2n + 1$ n_2	A	$0kl$: $k + l =$ $2n + 1$ n_1	A	$0kl$: $k + l =$ $2n + 1$ n_1 $h0l$: $h + l =$ $2n + 1$ n_2	A			$0kl$: $k + l =$ $2n + 1$ n_1	A_h	$h0l$: $h + l =$ $2n + 1$ n_2	A_h
59	$P2_1/m2_1/m2/n$	$hk0$: $h + k =$ $2n + 1$ n	A	$hk0$: $h + k =$ $2n + 1$ n	A			$hk0$: $h + k =$ $2n + 1$ n	A_h				
60	$P2_1/b2/c2_1/n$	$h0l_o$ c $hk0$: $h + k =$ $2n + 1$ n	A	$0k_ol$ b $hk0$: $h + k =$ $2n + 1$ n	A	$0k_ol$ b $h0l_o$ c	A	$hk0$: $h + k =$ $2n + 1$ n	A_h	$0k_ol$ b	A_h	$h0l_o$ c	A_h
61	$P2_1/b2_1/c2_1/a$	$h0l_o$ c h_ok0 a	A	$0k_ol$ b h_ok0 a	A	$0k_ol$ b $h0l_o$ c	A	h_ok0 a	A_h	$0k_ol$ b	A_h	$h0l_o$ c	A_h
62	$P2_1/n2_1/m2_1/a$	h_ok0 a	A	$0kl$: $k + l =$ $2n + 1$ n h_ok0 a	A	$0kl$: $k + l =$ $2n + 1$ n	A	h_ok0 a	A_h	$0kl$: $k + l =$ $2n + 1$ n	A_h		
63	$C2/m2/c2_1/m$	h_e0l_o c	A			h_e0l_o c	A					h_e0l_o c	A_h
64	$C2/m2/c2_1/a$	h_e0l_o c h_ok_o0 a	A	h_ok_o0 a	A	h_e0l_o c	A	h_ok_o0 a	A_h			h_e0l_o c	A_h
65	$C2/m2/m2/m$												
66	$C2/c2/c2/m$	h_e0l_o c_2	A	$0k_el_o$ c_1	A	$0k_el_o$ c_1 h_e0l_o c_2	A			$0k_el_o$ c_1	A_h	h_e0l_o c_2	A_h
67	$C2/m2/m2/a$	h_ok_o0 a	A	h_ok_o0 a	A			h_ok_o0 a	A_h				
68	$C2/c2/c2/a$	h_e0l_o c_2 h_ok_o0 a	A	$0k_el_o$ c_1 h_ok_o0 a	A	$0k_el_o$ c_1 h_e0l_o c_2	A	h_ok_o0 a	A_h	$0k_el_o$ c_1	A_h	h_e0l_o c_2	A_h
69	$F2/m2/m2/m$												
70	$F2/d2/d2/d$	h_e0l_e: $h_e + l_e =$ $4n + 2$ d_2 h_ek_e0: $h_e + k_e =$ $4n + 2$ d_3	A	h_ek_e0: $h_e + k_e =$ $4n + 2$ d_3 $0k_el_e$: $k_e + l_e =$ $4n + 2$ d_1	A	$0k_el_e$: $k_e + l_e =$ $4n + 2$ d_1 h_e0l_e: $h_e + l_e =$ $4n + 2$ d_2	A	h_ek_e0: $h_e + k_e =$ $4n + 2$ d_3	A_h	$0k_el_e$: $k_e + l_e =$ $4n + 2$ d_1	A_h	h_e0l_e: $h_e + l_e =$ $4n + 2$ d_2	A_h
71	$I2/m2/m2/m$												

Table 2.5.3.12 (*cont.*)

Space group		Incident-beam direction											
		[100]		[010]		[001]		[uv0]		[0vw]		[u0w]	
72	$I2/b2/a2/m$	h_o0l_o a	A	$0k_ol_o$ b	A	$0k_ol_o$ b h_o0l_o a	A			$0k_ol_o$ b	A_h	h_o0l_o a	A_h
73	$I2_1/b2_1/c2_1/a$	h_o0l_o c h_ok_o0 a	A	h_ok_o0 a $0k_ol_o$ b	A	$0k_ol_o$ b h_o0l_o c	A	h_ok_o0 a	A_h	$0k_ol_o$ b	A_h	h_o0l_o c	A_h
74	$I2_1/m2_1/m2_1/a$	h_ok_o0 a	A	h_ok_o0 a	A			h_ok_o0 a	A_h				

Point group 4/m

Space group		Incident-beam direction			
		[100], [110]		[uv0]	
83	$P4/m$				
84	$P4_2/m$				
85	$P4/n$	$hk0$: $h + k = 2n + 1$ n	A	$hk0$: $h + k = 2n + 1$ n	A_h
86	$P4_2/n$	$hk0$: $h + k = 2n + 1$ n	A	$hk0$: $h + k = 2n + 1$ n	A_h
87	$I4/m$				
88	$I4_1/a$	h_ok_o0 a	A	h_ok_o0 a	A_h

Point group 4mm. The symbol a in the column [u0w] is equivalent to the symbol b in the space groups of the first column.

Space group		Incident-beam direction									
		[100]		[001]		[110]		[u0w]		[uuw]	
99	$P4mm$										
100	$P4bm$	h_o0l a_2	A	$0k_ol$ b_1 h_o0l a_2	A			h_o0l a	A_h		
101	$P4_2cm$	$h0l_o$ c_2	A	$0kl_o$ c_1 $h0l_o$ c_2	A			$h0l_o$ c	A_h		
102	$P4_2nm$	$h0l$: $h + l = 2n + 1$ n_2	A	$0kl$: $k + l = 2n + 1$ n_1 $h0l$: $h + l = 2n + 1$ n_2	A			$h0l$: $h + l = 2n + 1$ n	A_h		
103	$P4cc$	$h0l_o$ c_{12}	A	$0kl_o$ c_{11} $h0l_o$ c_{12} $hhl_o, \bar{h}hl_o$ c_2	A	hhl_o c_2	A	$h0l_o$ c_1	A_h	hhl_o c_2	A_h
104	$P4nc$	$h0l$: $h + l = 2n + 1$ n_2	A	$0kl$: $k + l = 2n + 1$ n_1 $h0l$: $h + l = 2n + 1$ n_2 $hhl_o, \bar{h}hl_o$ c	A	hhl_o c	A	$h0l$: $h + l = 2n + 1$ n	A_h	hhl_o c	A_h
105	$P4_2mc$			$hhl_o, \bar{h}hl_o$ c	A	hhl_o c	A			hhl_o c	A_h
106	$P4_2bc$	h_o0l a_2	A	$0k_ol$ b_1 h_o0l a_2 $hhl_o, \bar{h}hl_o$ c	A	hhl_o c	A	h_o0l a	A_h	hhl_o c	A_h
107	$I4mm$										

Table 2.5.3.12 (*cont.*)

Space group		Incident-beam direction									
		[100]		[001]		[110]		[$u0w$]		[uuw]	
108	$I4cm$	h_o0l_o c_2	A	$0k_ol_o$ c_1 h_o0l_o c_2	A			h_o0l_o c	A_h		
109	$I4_1md$			hhl_e, $\bar{h}hl_e$: $2h + l_e = 4n + 2$ d	A	hhl_e: $2h + l_e = 4n + 2$ d	A			hhl_e: $2h + l_e = 4n + 2$ d	A_h
110	$I4_1cd$	h_o0l_o c_2	A	$0k_ol_o$ c_1 h_o0l_o c_2 hhl_e, $\bar{h}hl_e$: $2h + l_e = 4n + 2$ d	A	hhl_e: $2h + l_e = 4n + 2$ d	A	h_o0l_o c	A_h	hhl_e: $2h + l_e = 4n + 2$ d	A_h

Point group $\bar{4}2m$. The symbol a in the column [$u0w$] is equivalent to the symbol b in the space groups of the first column.

Space group		Incident-beam direction									
		[100]		[001]		[110]		[$u0w$]		[uuw]	
111	$P\bar{4}2m$										
112	$P\bar{4}2c$			hhl_o, $\bar{h}hl_o$ c	A	hhl_o c	A			hhl_o c	A_h
113	$P\bar{4}2_1m$										
114	$P\bar{4}2_1c$			hhl_o, $\bar{h}hl_o$ c	A	hhl_o c	A			hhl_o c	A_h
115	$P\bar{4}m2$										
116	$P\bar{4}c2$	$h0l_o$ c_2	A	$0kl_o$ c_1 $h0l_o$ c_2	A			$h0l_o$ c	A_h		
117	$P\bar{4}b2$	h_o0l a_2	A	$0k_ol$ b_1 h_o0l a_2	A			h_o0l a	A_h		
118	$P\bar{4}n2$	$h0l$: $h + l = 2n + 1$ n_2	A	$0kl$: $k + l = 2n + 1$ n_1 $h0l$: $h + l = 2n + 1$ n_2	A			$h0l$: $h + l = 2n + 1$ n	A_h		
119	$I\bar{4}m2$										
120	$I\bar{4}c2$	h_o0l_o c_2	A	$0k_ol_o$ c_1 h_o0l_o c_2	A			h_o0l_o c	A_h		
121	$I\bar{4}2m$										
122	$I\bar{4}2d$			hhl_e, $\bar{h}hl_e$: $2h + l_e = 4n + 2$ d	A	hhl_e: $2h + l_e = 4n + 2$ d	A			hhl_e: $2h + l_e = 4n + 2$ d	A_h

Point group $4/mmm$. The symbol a in the column [$u0w$] is equivalent to the symbol b in the space groups of the first column.

Space group		Incident-beam direction											
		[100]		[001]		[110]		[$u0w$]		[uuw]		[$uv0$]	
123	$P4/mmm$ $P4/m2/m2/m$												
124	$P4/mcc$ $P4/m2/c2/c$	$h0l_o$ c_{12}	A	$0kl_o$ c_{11} $h0l_o$ c_{12} hhl_o, $\bar{h}hl_o$ c_2	A	hhl_o c_2	A	$h0l_o$ c_1	A_h	hhl_o c_2	A_h		
125	$P4/nbm$ $P4/n2/b2/m$	$hk0$: $h + k =$ $2n + 1$ n h_o0l a_2	A	$0k_ol$ b_1 h_o0l a_2	A	$hk0$: $h + k =$ $2n + 1$ n	A	h_o0l a	A_h			$hk0$: $h + k =$ $2n + 1$ n	A_h

Table 2.5.3.12 (*cont.*)

Space group		Incident-beam direction											
		[100]		[001]		[110]		[u0w]		[uuw]		[uv0]	
126	*P*4/*nnc* *P*4/*n*2/*n*2/*c*	$hk0$: $h + k =$ $2n + 1$ n_1 $h0l$: $h + l =$ $2n + 1$ n_{22}	A	$0kl$: $k + l =$ $2n + 1$ n_{21} $h0l$: $h + l =$ $2n + 1$ n_{22} $hhl_o, \bar{h}hl_o$ c	A	$hk0$: $h + k =$ $2n + 1$ n_1 hhl_o c	A	$h0l$: $h + l =$ $2n + 1$ n_2	A_h	hhl_o c	A_h	$hk0$: $h + k =$ $2n + 1$ n_1	A_h
127	*P*4/*mbm* *P*4/*m*2$_1$/*b*2/*m*	h_o0l a_2	A	$0k_ol$ b_1 h_o0l a_2	A			h_o0l a	A_h				
128	*P*4/*mnc* *P*4/*m*2$_1$/*n*2/*c*	$h0l$: $h + l =$ $2n + 1$ n_2	A	$0kl$: $k + l =$ $2n + 1$ n_1 $h0l$: $h + l =$ $2n + 1$ n_2 $hhl_o, \bar{h}hl_o$ c	A	hhl_o c	A	$h0l$: $h + l =$ $2n + 1$ n	A_h	hhl_o c	A_h		
129	*P*4/*nmm* *P*4/*n*2$_1$/*m*2/*m*	$hk0$: $h + k =$ $2n + 1$ n	A			$hk0$: $h + k =$ $2n + 1$ n	A					$hk0$: $h + k =$ $2n + 1$ n	A_h
130	*P*4/*ncc* *P*4/*n*2$_1$/*c*2/*c*	$hk0$: $h + k =$ $2n + 1$ n $h0l_o$ c_{12}	A	$0kl_o$ c_{11} $h0l_o$ c_{12} $hhl_o, \bar{h}hl_o$ c_2	A	$hk0$: $h + k =$ $2n + 1$ n hhl_o c_2	A	$h0l_o$ c_1	A_h	hhl_o c_2	A_h	$hk0$: $h + k =$ $2n + 1$ n	A_h
131	*P*4$_2$/*mmc* *P*4$_2$/*m*2/*m*2/*c*			$hhl_o, \bar{h}hl_o$ c	A	hhl_o c	A			hhl_o c	A_h		
132	*P*4$_2$/*mcm* *P*4$_2$/*m*2/*c*2/*m*	$h0l_o$ c_2	A	$0kl_o$ c_1 $h0l_o$ c_2	A			$h0l_o$ c	A_h				
133	*P*4$_2$/*nbc* *P*4$_2$/*n*2/*b*2/*c*	$hk0$: $h + k =$ $2n + 1$ n h_o0l a_2	A	$0k_ol$ b_1 h_o0l a_2 $hhl_o, \bar{h}hl_o$ c	A	$hk0$: $h + k =$ $2n + 1$ n hhl_o c	A	h_o0l a	A_h	hhl_o c	A_h	$hk0$: $h + k =$ $2n + 1$ n	A_h
134	*P*4$_2$/*nnm* *P*4$_2$/*n*2/*n*2/*m*	$hk0$: $h + k =$ $2n + 1$ n_1 $h0l$: $h + l =$ $2n + 1$ n_{22}	A	$0kl$: $k + l =$ $2n + 1$ n_{21} $h0l$: $h + l =$ $2n + 1$ n_{22}	A	$hk0$: $h + k =$ $2n + 1$ n_1	A	$h0l$: $h + l =$ $2n + 1$ n_2	A_h			$hk0$: $h + k =$ $2n + 1$ n_1	A_h
135	*P*4$_2$/*mbc* *P*4$_2$/*m*2$_1$/*b*2/*c*	h_o0l a_2	A	$0k_ol$ b_1 h_o0l a_2 $hhl_o, \bar{h}hl_o$ c	A	hhl_o c	A	h_o0l a	A_h	hhl_o c	A_h		
136	*P*4$_2$/*mnm* *P*4$_2$/*m*2$_1$/*n*2/*m*	$h0l$: $h + l =$ $2n + 1$ n_2	A	$0kl$: $k + l =$ $2n + 1$ n_1 $h0l$: $h + l =$ $2n + 1$ n_2	A			$h0l$: $h + l =$ $2n + 1$ n	A_h				

Table 2.5.3.12 (*cont.*)

Space group		Incident-beam direction											
		[100]		[001]		[110]		[*u*0*w*]		[*uuw*]		[*uv*0]	
137	$P4_2/nmc$ $P4_2/n2_1/m2/c$	$hk0$: $h + k = 2n + 1$ n	A	hhl_o, $\bar{h}hl_o$ c	A	hhl_o c $hk0$: $h + k = 2n + 1$ n	A			hhl_o c	A_h	$hk0$: $h + k = 2n + 1$ n	A_h
138	$P4_2/ncm$ $P4_2/n2_1/c2/m$	$hk0$: $h + k = 2n + 1$ n $h0l_o$ c_2	A	$0kl_o$ c_1 $h0l_o$ c_2	A	$hk0$: $h + k = 2n + 1$ n	A	$h0l_o$ c	A_h			$hk0$: $h + k = 2n + 1$ n	A_h
139	$I4/mmm$ $I4/m2/m2/m$												
140	$I4/mcm$ $I4/m2/c2/m$	h_o0l_o c_2	A	$0k_ol_o$ c_1 h_o0l_o c_2	A			h_o0l_o c	A_h				
141	$I4_1/amd$ $I4_1/a2/m2/d$	h_ok_o0 a	A	hhl_e, $\bar{h}hl_e$: $2h + l_e = 4n + 2$ d	A	h_ok_o0 a hhl_e: $2h + l_e = 4n + 2$ d	A			hhl_e: $2h + l_e = 4n + 2$ d	A_h	h_ok_o0 a	A_h
142	$I4_1/acd$ $I4_1/a2/c2/d$	h_ok_o0 a h_o0l_o c_2	A	$0k_ol_o$ c_1 h_o0l_o c_2 hhl_e, $\bar{h}hl_e$: $2h + l_e = 4n + 2$ d	A	h_ok_o0 a hhl_e: $2h + l_e = 4n + 2$ d	A	h_o0l_o c	A_h	hhl_e: $2h + l_e = 4n + 2$ d	A_h	h_ok_o0 a	A_h

Point groups $3m$, $\bar{3}m$

Space group		Incident-beam direction									
		[0001]		[11$\bar{2}$0]		[1$\bar{1}$00]		[11$\bar{2}w$]		[1$\bar{1}0w$]	
156	$P3m1$										
157	$P31m$										
158	$P3c1$	$h\bar{h}0l_o$, $0h\bar{h}l_o$, $\bar{h}0hl_o$ c	A			$h\bar{h}0l_o$ c	A			$h\bar{h}0l_o$ c	A_h
159	$P31c$	$hh\overline{2h}l_o$, $h\overline{2h}hl_o$, $\overline{2h}hhl_o$ c	A	$hh\overline{2h}l_o$ c	A			$hh\overline{2h}l_o$ c	A_h		
160	$R3m$										
161	$R3c$	$h\bar{h}0l_o$, $0h\bar{h}l_o$, $\bar{h}0hl_o$: $h + l_o = 3n$ c	A_h			$h\bar{h}0l_o$: $h + l_o = 3n$ c	A_h			$h\bar{h}0l_o$: $h + l_o = 3n$ c	A_h
162	$P\bar{3}1m$										
163	$P\bar{3}1c$	$hh\overline{2h}l_o$, $h\overline{2h}hl_o$, $\overline{2h}hhl_o$ c	A	$hh\overline{2h}l_o$ c	A			$hh\overline{2h}l_o$ c	A_h		
164	$P\bar{3}m1$										
165	$P\bar{3}c1$	$h\bar{h}0l_o$, $0h\bar{h}l_o$, $\bar{h}0hl_o$ c	A			$h\bar{h}0l_o$ c	A			$h\bar{h}0l_o$ c	A_h
166	$R\bar{3}m$										
167	$R\bar{3}c$	$h\bar{h}0l_o$, $0h\bar{h}l_o$, $\bar{h}0hl_o$: $h + l_o = 3n$ c	A_h			$h\bar{h}0l_o$: $h + l_o = 3n$ c	A_h			$h\bar{h}0l_o$: $h + l_o = 3n$ c	A_h

Point groups $6mm$, $\bar{6}m2$, $6/mmm$

Space group		Incident-beam direction									
		[0001]		[11$\bar{2}$0]		[1$\bar{1}$00]		[11$\bar{2}w$]		[1$\bar{1}0w$]	
183	$P6mm$										
184	$P6cc$	$h\bar{h}0l_o$, $0h\bar{h}l_o$, $\bar{h}0hl_o$ c_1 $hh\overline{2h}l_o$, $h\overline{2h}hl_o$, $\overline{2h}hhl_o$ c_2	A	$hh\overline{2h}l_o$ c_2	A	$h\bar{h}0l_o$ c_1	A	$hh\overline{2h}l_o$ c_2	A_h	$h\bar{h}0l_o$ c_1	A_h

Table 2.5.3.12 (*cont.*)

Space group		Incident-beam direction									
		[0001]		[11$\bar{2}$0]		[1$\bar{1}$00]		[11$\bar{2}$*w*]		[1$\bar{1}$0*w*]	
185	*P*6$_3$*cm*	$hh\bar{2}\bar{h}l_o, h\bar{2}\bar{h}hl_o, \bar{2}\bar{h}hhl_o$ *c*	*A*			$h\bar{h}0l_o$ *c*	*A*			$h\bar{h}0l_o$ *c*	A_h
186	*P*6$_3$*mc*	$hh\bar{2}\bar{h}l_o, h\bar{2}\bar{h}hl_o, \bar{2}\bar{h}hhl_o$ *c*	*A*	$hh\bar{2}\bar{h}l_o$ *c*	*A*			$hh\bar{2}\bar{h}l_o$ *c*	A_h		
187	*P*$\bar{6}$*m*2										
188	*P*$\bar{6}$*c*2	$h\bar{h}0l_o, 0h\bar{h}l_o, \bar{h}0hl_o$ *c*	*A*			$h\bar{h}0l_o$ *c*	*A*			$h\bar{h}0l_o$ *c*	A_h
189	*P*$\bar{6}$2*m*										
190	*P*$\bar{6}$2*c*	$hh\bar{2}\bar{h}l_o, h\bar{2}\bar{h}hl_o, \bar{2}\bar{h}hhl_o$ *c*	*A*	$hh\bar{2}\bar{h}l_o$ *c*	*A*			$hh\bar{2}\bar{h}l_o$ *c*	A_h		
191	*P*6/*mmm*										
192	*P*6/*mcc*	$h\bar{h}0l_o, 0h\bar{h}l_o, \bar{h}0hl_o$ c_1 $hh\bar{2}\bar{h}l_o, h\bar{2}\bar{h}hl_o, \bar{2}\bar{h}hhl_o$ c_2	*A*	$hh\bar{2}\bar{h}l_o$ c_2	*A*	$h\bar{h}0l_o$ c_1	*A*	$hh\bar{2}\bar{h}l_o$ c_2	A_h	$h\bar{h}0l_o$ c_1	A_h
193	*P*6$_3$/*mcm*	$h\bar{h}0l_o, 0h\bar{h}l_o, \bar{h}0hl_o$ *c*	*A*			$h\bar{h}0l_o$ *c*	*A*			$h\bar{h}0l_o$ *c*	A_h
194	*P*6$_3$/*mmc*	$hh\bar{2}\bar{h}l_o, h\bar{2}\bar{h}hl_o, \bar{2}\bar{h}hhl_o$ *c*	*A*	$hh\bar{2}\bar{h}l_o$ *c*	*A*			$hh\bar{2}\bar{h}l_o$ *c*	A_h		

Point group *m*3

Space group		Incident-beam direction					
		[100]		[110]		[*uv*0]	
200	*Pm*3 *P*2/*m*$\bar{3}$						
201	*Pn*3 *P*2/*n*$\bar{3}$	*h*0*l*: $h + l = 2n + 1$ n_2 *hk*0: $h + k = 2n + 1$ n_3	*A*	*hk*0: $h + k = 2n + 1$ n_3	*A*	*hk*0: $h + k = 2n + 1$ *n*	A_h
202	*Fm*3 *F*2/*m*$\bar{3}$						
203	*Fd*3 *F*2/*d*$\bar{3}$	h_e0l_e: $h_e + l_e = 4n + 2$ d_2 h_ek_e0: $h_e + k_e = 4n + 2$ d_3	*A*	h_ek_e0: $h_e + k_e = 4n + 2$ d_3	*A*	h_ek_e0: $h_e + k_e = 4n + 2$ *d*	A_h
204	*Im*3 *I*2/*m*$\bar{3}$						
205	*Pa*3 *P*2$_1$/*a*$\bar{3}$	$h0l_o$ c_2 h_ok0 a_3	*A*	h_ok0 a_3	*A**	h_ok0 *a*	A_h
206	*Ia*3 *I*2$_1$/*a*$\bar{3}$	h_o0l_o c_2 h_ok_o0 a_3	*A*	h_ok_o0 a_3	*A*	h_ok_o0 *a*	A_h

Point group $\bar{4}3m$. The symbol *a* in the column [100] is equivalent to the symbol *c* in the space groups of the first column.

Space group		Incident-beam direction					
		[100]		[110]		[*uuw*]	
215	*P*$\bar{4}$3*m*						
216	*F*$\bar{4}$3*m*						
217	*I*$\bar{4}$3*m*						
218	*P*$\bar{4}$3*n*	$h_okk, h_o\bar{k}k$ *n*	*A*	hhl_o *n*	*A*	hhl_o *n*	A_h
219	*F*$\bar{4}$3*c*	$h_ok_ok_o, h_o\bar{k}_ok_o$ *a*	*A*	$h_oh_ol_o$ *c*	*A*	$h_oh_ol_o$ *c*	A_h
220	*I*$\bar{4}$3*d*	$h_ekk, h_e\bar{k}k$: $2k + h_e = 4n + 2$ *d*	*A*	hhl_e: $2h + l_e = 4n + 2$ *d*	*A*	hhl_e: $2h + l_e = 4n + 2$ *d*	A_h

Table 2.5.3.12 (*cont.*)

Point group $m3m$. The symbol a in the column [100] is equivalent to the symbol c in the space groups of the first column.

Space group		Incident-beam direction							
		[100]		[110]		[uv0]		[uuw]	
221	$Pm\bar{3}m$ $P4/m\bar{3}2/m$								
222	$Pn\bar{3}n$ $P4/n\bar{3}2/n$	$h0l$: $h + l = 2n + 1$ n_{12} $hk0$: $h + k = 2n + 1$ n_{13} $h_{\rm o}kk, h_{\rm o}\bar{k}k$ n_2	A	$hk0$: $h + k = 2n + 1$ n_{13} $hhl_{\rm o}$ n_2	A	$hk0$: $h + k = 2n + 1$ n_1	$A_{\rm h}$	$hhl_{\rm o}$ n_2	$A_{\rm h}$
223	$Pm\bar{3}n$ $P4_2/m\bar{3}2/n$	$h_{\rm o}kk, h_{\rm o}\bar{k}k$ n	A	$hhl_{\rm o}$ n	A			$hhl_{\rm o}$ n	$A_{\rm h}$
224	$Pn\bar{3}m$ $P4_2/n\bar{3}2/m$	$h0l$: $h + l = 2n + 1$ n_2 $hk0$: $h + k = 2n + 1$ n_3	A	$hk0$: $h + k = 2n + 1$ n_3	A	$hk0$: $h + k = 2n + 1$ n	$A_{\rm h}$		
225	$Fm\bar{3}m$ $F4/m\bar{3}2/m$								
226	$Fm\bar{3}c$ $F4/m\bar{3}2/c$	$h_{\rm o}k_{\rm o}k_{\rm o}, h_{\rm o}\bar{k}_{\rm o}k_{\rm o}$ a	A	$h_{\rm o}h_{\rm o}l_{\rm o}$ c	A			$h_{\rm o}h_{\rm o}l_{\rm o}$ c	$A_{\rm h}$
227	$Fd\bar{3}m$ $F4_1/d\bar{3}2/m$	$h_{\rm e}0l_{\rm e}$: $h_{\rm e} + l_{\rm e} = 4n + 2$ d_2 $h_{\rm e}k_{\rm e}0$: $h_{\rm e} + k_{\rm e} = 4n + 2$ d_3	A	$h_{\rm e}k_{\rm e}0$: $h_{\rm e} + k_{\rm e} = 4n + 2$ d_3	A	$h_{\rm e}k_{\rm e}0$: $h_{\rm e} + k_{\rm e} = 4n + 2$ d	$A_{\rm h}$		
228	$Fd\bar{3}c$ $F4_1/d\bar{3}2/c$	$h_{\rm e}0l_{\rm e}$: $h_{\rm e} + l_{\rm e} = 4n + 2$ d_2 $h_{\rm e}k_{\rm e}0$: $h_{\rm e} + k_{\rm e} = 4n + 2$ d_3 $h_{\rm o}k_{\rm o}k_{\rm o}, h_{\rm o}\bar{k}_{\rm o}k_{\rm o}$ a	A	$h_{\rm o}h_{\rm o}l_{\rm o}$ c $h_{\rm e}k_{\rm e}0$: $h_{\rm e} + k_{\rm e} = 4n + 2$ d_3	A	$h_{\rm e}k_{\rm e}0$: $h_{\rm e} + k_{\rm e} = 4n + 2$ d	$A_{\rm h}$	$h_{\rm o}h_{\rm o}l_{\rm o}$ c	$A_{\rm h}$
229	$Im\bar{3}m$ $I4/m\bar{3}2/m$								
230	$Ia\bar{3}d$ $I4_1/a\bar{3}2/d$	$h_{\rm o}k_{\rm o}0$ a_3 $h_{\rm o}0l_{\rm o}$ c_2 $h_{\rm e}kk, h_{\rm e}\bar{k}k$: $2k + h_{\rm e} = 4n + 2$ d	A	$hhl_{\rm e}$: $2h + l_{\rm e} = 4n + 2$ d $h_{\rm o}k_{\rm o}0$ a_3	A	$h_{\rm o}k_{\rm o}0$ a	$A_{\rm h}$	$hhl_{\rm e}$: $2h + l_{\rm e} = 4n + 2$ d	$A_{\rm h}$

are no kinematically forbidden reflections. Thus, the lattice type is determined to be primitive P.

Possible space groups which satisfy point group $4/mmm$ and primitive lattice type P are those of Nos. 123–138 in Table 2.5.3.9. In Fig. 2.5.3.15(a), the dynamical extinction line A_2 is seen in the 100 disc and in the equivalent 010 disc. By consulting Table 2.5.3.9, four space groups $P4/mbm$, $P4/mnc$, $P4_2/mbc$ and $P4_2/mnm$ are selected. In Fig. 2.5.3.15(b), the dynamical extinction line A_2 is seen in the 010 disc but not in the $10\bar{1}$ disc. Two space groups $P4/mnc$ and $P4_2/mnm$ are selected from the four. To distinguish the two space groups, it is found from Table 2.5.3.9 that a CBED pattern taken with the [110] electron incidence should be examined. Fig. 2.5.3.15(e) shows a CBED pattern taken with the [110] incidence at 100 kV, where the 001 reflection is exactly excited. The $hh\bar{1}$ reflections are kinematically allowed for space group $P4_2/mnm$ but kinematically forbidden for $P4/mnc$. Since in the case of $P4/mnc$, no *Umweganregung* (multiple scattering) paths to the 001 reflection exist in the zeroth-order Laue zone, only the intensities of HOLZ lines, which are caused by *Umweganregung via* HOLZ reflections, are expected to appear in the 001 disc. If such *Umweganregung* is not practically excited, the 001 reflection must have no intensity. However, strong intensity produced by two-dimensional interaction is seen in the 001 disc of Fig. 2.5.3.15(e). This indicates that the reflection is an allowed reflection. Therefore, the space group of rutile is determined to be $P4_2/mnm$, which agrees with the space group already known.

Samarium selenide (Sm_3Se_4). Sm_3Se_4 has the Th_3P_4 structure type with space group $I\bar{4}3d$ at high temperatures. The lattice parameters are $a = b = c = 0.8885$ nm. It was expected that Sm_3Se_4 would transform to an ordered state of electrons with two valences of +2 and +3 around 150 K. The determination of the space group of the material was conducted at 100 K and room temperature. The space groups at both temperatures were determined by CBED to be the same. The following experiments were performed at 100 K.

Fig. 2.5.3.16(a) shows a CBED pattern taken with the [111] incidence at 80 kV, which clearly shows the first-order-Laue-zone reflections. The symmetry of the WP is seen to be $3m$ with the help of the enlarged insets. Possible diffraction groups are $3m$, $3m1_R$ and 6_Rmm_R from Table 2.5.3.3. Fig. 2.5.3.16(b), which is the central part of Fig. 2.5.3.16(a), shows projection symmetry $3m$, indicating that the projection diffraction group is $3m1_R$. Among the three groups $3m$, $3m1_R$ and 6_Rmm_R, diffraction groups for which the projection diffraction group is $3m1_R$ are $\bar{3}m$ and $3m1_R$. Possible point groups are found to be $3m$, $\bar{4}3m$ and $\bar{6}m2$ from Fig. 2.5.3.4. Fig. 2.5.3.16(c) shows a CBED pattern taken with the [100] incidence at 80 kV. The WP is seen to have symmetry $2mm$. Allowed diffraction groups are $2mm$, $2mm1_R$ and 4_Rmm_R. Fig. 2.5.3.16(d), which is the central part of Fig. 2.5.3.16(c), shows projection WP symmetry $4mm$, indicating that the projection diffraction group is $4mm1_R$. The diffraction group among the three groups $2mm$, $2mm1_R$ and 4_Rmm_R whose projection diffraction group is $4mm1_R$ is 4_Rmm_R. Possible point groups are found to be $\bar{4}3m$ and $\bar{4}2m$ from Fig. 2.5.3.4. Thus, the point group

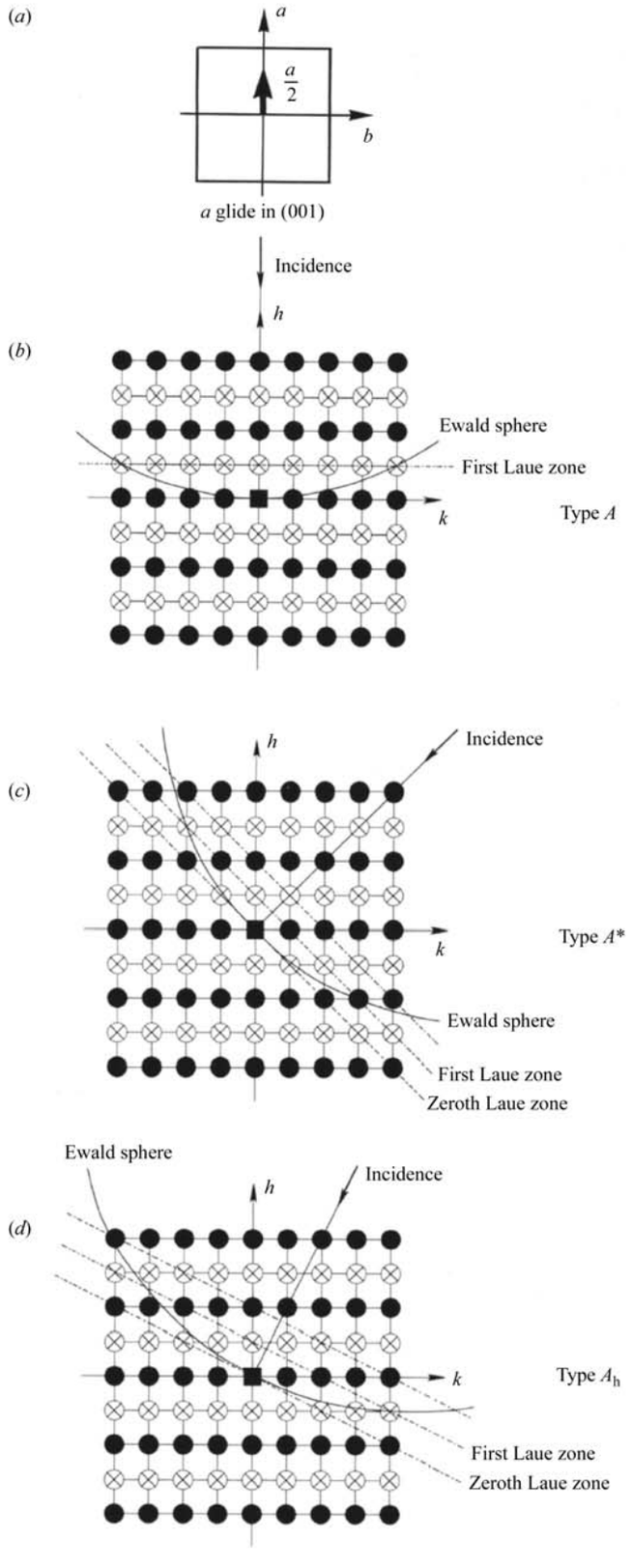

Fig. 2.5.3.13. Illustration of dynamical extinction lines appearing in HOLZ reflections due to glide planes. Black circles and circled crosses show kinematically allowed and kinematically forbidden reflections, respectively. (*a*) *a* glide in the (001) plane. (*b*) [100] incidence: dynamical extinction lines are formed in HOLZ reflections on both sides of the incident beam (type *A*). (*c*) [110] incidence: an extinction line is formed at a HOLZ reflection on one side of the incident beam because on the other side the Ewald sphere intersects an allowed HOLZ reflection (type *A**). (*d*) An incidence between [100] and [110]: an extinction line is formed at a HOLZ reflection on one side of the incident beam because on the other side the Ewald sphere does not intersect a HOLZ reflection (type A_h).

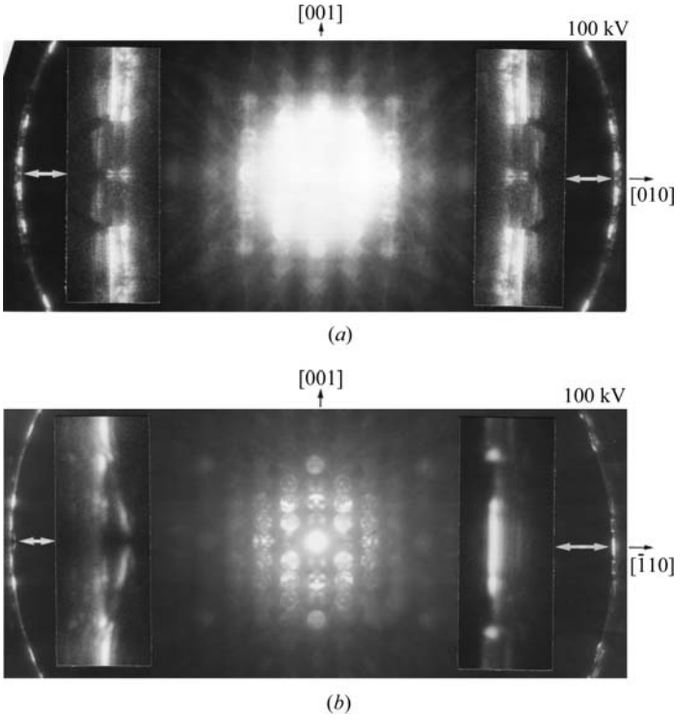

Fig. 2.5.3.14. HOLZ CBED pattern of FeS_2. (*a*) [100] incidence: type *A* dynamical extinction lines are seen clearly in the enlarged insets. (*b*) [110] incidence: a type *A** dynamical extinction line is seen clearly in the enlarged insets.

which satisfies the results obtained at the two crystal orientations is $\bar{4}3m$.

Fig. 2.5.3.16(*e*) shows an ordinary diffraction pattern taken with the [100] incidence at 80 kV. With the help of the lattice parameters and the camera length, the indices of the reflections are given as shown in the figure. The reflections $0kl$ ($k + l = 2n + 1$) are found to be kinematically forbidden. Thus, the lattice type is determined to be *I*.

The space groups having point group $\bar{4}3m$ and lattice type *I* are $I\bar{4}3m$ and $I\bar{4}3d$ from Table 2.5.3.9. Fig. 2.5.3.16(*d*) shows dynamical extinction lines A_2 in the 033 disc and equivalent discs (also broad lines A_2 in the 011 discs). Since the former space group does not give any dynamical extinction lines, the space group is determined to be $I\bar{4}3d$. For confirmation, a CBED pattern which contains the second-order-Laue-zone reflections was taken (Fig. 2.5.3.16*f*). Dynamical extinction lines *A* are seen in the 2,22,22 disc and the equivalent discs. This result also identifies the space group to be not $I\bar{4}3m$ but $I\bar{4}3d$ with the aid of Table 2.5.3.12.

2.5.3.4. Symmetry determination of incommensurate crystals

2.5.3.4.1. General remarks

Incommensurately modulated crystals do not have three-dimensional lattice periodicity. The crystals, however, recover lattice periodicity in a space higher than three dimensions. de Wolff (1974, 1977) showed that one-dimensional displacive and substitutionally modulated crystals can be described as a three-dimensional section of a (3 + 1)-dimensional periodic crystal. Janner & Janssen (1980*a*,*b*) developed a more general approach for describing a modulated crystal with *n* modulations as (3 + *n*)-dimensional periodic crystals ($n = 1, 2, \ldots$). Yamamoto (1982) derived a general structure-factor formula for *n*-dimensionally modulated crystals ($n = 1, 2, \ldots$), which holds for both displacive and substitutionally modulated crystals. Tables of the (3 + 1)-dimensional space groups for one-dimensional incommensurately modulated crystals were given by de Wolff *et al.* (1981), where the wavevector of the modulation was assumed to lie in the